63-3-2

ASD-TDR-62-492
Volume II

THEORETICAL INVESTIGATION OF A MAGNETO-OPTICAL GYROSCOPE

Alternatives to the Faraday Effect

TECHNICAL DOCUMENTARY REPORT NO. ASD-TDR-62-492, Volume II

February 1963

Navigation and Guidance Laboratory
Aeronautical Systems Division
Air Force Systems Command
Wright-Patterson Air Force Base, Ohio

Project No. 4431, Task No. 443124

(Prepared under Contract No. AF33(616)-7668
by Electronic Systems Laboratory,
Department of Electrical Engineering,
Massachusetts Institute of Technology,
Cambridge 39, Massachusetts)

NOTICES

When Government drawings, specifications, or other data are used for any purpose other than in connection with a definitely related Government procurement operation, the United States Government thereby incurs no responsibility nor any obligation whatsoever; and the fact that the Government may have formulated, furnished, or in any way supplied the said drawings, specifications, or other data, is not to be regarded by implication or otherwise as in any manner licensing the holder or any other person or corporation, or conveying any rights or permission to manufacture, use, or sell any patented invention that may in any way be related thereto.

ASTIA release to OTS not authorized.

Qualified requesters may obtain copies of this report from the Armed Services Technical Information Agency, (ASTIA), Arlington Hall Station, Arlington 12, Virginia.

All of the items compared in this report were commercial items that were not developed or manufactured to meet any Government specification, to withstand the tests to which they were subjected, or to operate as applied during this study. Any failure to meet objectives of this study is no reflection on any of the commercial items discussed herein. This report shall not be considered as an endorsement of any item. The report shall not be used for advertising purposes by any organization.

Copies of this report should not be returned to the Aeronautical Systems Division unless return is required by security considerations, contractual obligations, or notice on a specific document.

24-560N, 300, 4-11-63

FOREWORD

This report was prepared by the Electronic Systems Laboratory, Massachusetts Institute of Technology Cambridge 39, Massachusetts, on Air Force Contract AF-33(616)-7668 under Task No. 443124 of Project No. 4431 (formerly 50758 and 1 (620-4431), respectively). The work was administered under the direction of the Navigation and Guidance Laboratory, Aeronautical Systems Division. Captain James E. Stevens (ASRNGC-2) was project engineer for the Navigation and Guidance Laboratory.

This report, in two volumes of which this is Volume II, is the Technical Documentary Report that constitutes Item II under Contract No. AF 33(616)-7668. The study covered by this report took place in the period November 1960 through April 1962. The contractor's report number is ESL-R-125(II).

The following professional staff members contributed to the research reported in this document:

R. Kramer	Project Engineer (to Feb. 1962)
G. C. Newton Jr.	Associate Professor of Electrical Engineering and Associate Director of the Electronic Systems Laboratory
P. S. Pershan	Consultant in Physics
G. Pollon	Research Assistant
R. B. Rothrock	Research Assistant
J. G. Whitman Jr.	Research Assistant

All of the above staff members contributed to the writing of this report.

ABSTRACT

This report summarizes a theoretical investigation of the feasibility of using magneto-optical and certain other physical phenomena for gyroscopic measurement purposes. The phenomena investigated in this report are nuclear angular momentum effects, Coriolis force effects on various particles and bulk fluid effects. This report supplements Report ESL-R-125-(I) which presents results of an investigation of magneto-optical and other closely related phenomena. The over-all investigation, including the researches of both the previous report and this supplement, is summarized in Chapter I of this report.

The conclusions reached are as follows. The magneto-optical gyroscope, based on the Barnett and Faraday effects, is potentially capable of a resolution on the order of 0.1 radian per second providing stray magnetic field effects are shielded to maintain field fluctuations down to the order of 10^{-9} gauss. Methods based on nuclear angular momentum may be able to achieve one to three orders of magnitude more resolution with less sensitivity to stray fields than the magneto-optical approach. Maser techniques would be needed to reach the lower limit on resolution. Coriolis force effects in specially constructed dielectrics appear to be too small in comparison with other forces to be useful. This conclusion applies to both microscopic and colloidal particle sizes. The investigation closed with a study of bulk fluid effects. It is shown that an ordinary liquid like mercury is sufficiently decoupled from its container so that it may be useful as a stable platform reference. However, the problem of measuring the displacement of the inner fluid mass with respect to its container has not been solved.

PUBLICATION REVIEW

This technical documentary report has been reviewed and is approved.

FOR THE COMMANDER:

DAVID K. DEAN
Colonel, USAF
Chief, Navigation &
Guidance Laboratory

TABLE OF CONTENTS

CHAPTER I	INTRODUCTION AND SUMMARY	page 1
	A. BACKGROUND AND OBJECTIVES	1
	B. METHODS OF APPROACH	1
	1. Barnett-Faraday Effect	2
	2. Nuclear Angular Momentum Effects	5
	3. Coriolis Force Effects with Small Particles	8
	4. Bulk Fluid Effects	10
	C. CONCLUSIONS	12
CHAPTER II	NUCLEAR ANGULAR MOMENTUM SENSOR	19
	A. INTRODUCTION	19
	B. NUCLEAR FREE GYRO	20
	C. CW NUCLEAR GYROSCOPES	31
	1. General Description	31
	2. Passive Devices	32
	3. Active Devices	39
	D. MAGNETIC SHIELDING	41
	E. CONCLUSION	43
CHAPTER III	MICROSCOPIC CORIOLIS FORCE SENSORS	45
	A. INTRODUCTION	45
	B. MOLECULAR SYSTEMS	46
	1. Bound Particles	46
	2. Free Particles	49
	3. Conclusions	53
	C. COLLOIDS	53
	D. CONCLUSION	58

TABLE OF CONTENTS (continued)

CHAPTER IV	FLUID GYRO	page	59
	A. INTRODUCTION		59
	B. ANALYSIS		60
	C. KINEMATIC VISCOSITY		64
	D. DEVICE CONFIGURATIONS--OPEN AND CLOSED LOOP OPERATION		66
	E. LOWER BOUND ON DETECTABLE RATE		71
	F. SUMMARY OF DEVICE PERFORMANCE		72
	G. CONCLUSIONS		74
REFERENCES			77

LIST OF FIGURES

3. 1	Simple Model for a Polar Solid	page	46
3. 2	Simple Model for a Polar Fluid		50
3. 3	Colloidal Particle		54
3. 4	Device Utilizing Colloidal Particles		56
4. 1	Geometry and Equations of Motion		60
4. 2	Fluid System Step Response		63
4. 3	Fluid System Frequency Response		63
4. 4	Kinematic Viscosities of Some Interesting Liquids		66
4. 5	Standard Notation for Angles		67
4. 6	Second Order Approximation to Open-Loop Response		68
4. 7	Open-Loop Response to a Constant Angular Rate		69
4. 8	A Possible Configuration for Closed-Loop Operation		70

CHAPTER I

INTRODUCTION AND SUMMARY

A. BACKGROUND AND OBJECTIVES

The mechanical gyroscope is currently the principal instrument used for inertial reference and inertial angular motion measurement. In free, gimballed configurations it provides angular position references and in restrained configurations it can provide angular rate information--all with respect to an inertial coordinate system. Gyroscopes enjoy a wide range of performance and application. Applications range from feedback stabilization of dynamic systems to high-precision, long-range navigation. In the most refined instruments the level of performance as measured by random drifts has been pushed to orders of magnitude below the angular rate of rotation of the earth which is about 10^{-4} rad/sec. This performance is the result of a tremendous development effort and is not achieved without great complexity and cost. Furthermore, there are some who feel that these high performance gyroscopic reference systems are very close to the ultimate performance that may be achieved.

In the light of these and other factors, there has been a series of parallel, relatively low level programs for investigating approaches other than those based upon a rotating wheel. In this report the results of one such effort are summarized. This comprises looking into the possible uses of some of the fundamental properties of materials to provide inertial reference data. The goal of the work was not limited to a particular type of inertial reference (positional or rate) but, rather, encompassed a general exploration of possible physical phenomena that might be useful for gyroscopic purposes.

B. METHODS OF APPROACH

In order to evaluate the potential of devices based on these novel principles, an angular rate equal to that of the earth's rotation--of the order of 10^{-4}--was selected as a measure of the performance desired. This figure would represent the drift rate of a position reference or the resolution of a rate reference. For each phenomenon studied an attempt was made to determine the output signal

Manuscript released by the authors in April 1962 for publication as an ASD Technical Documentary Report

level and signal-to-noise ratio for an earth's rate input. The various phenomena which were investigated include the Barnett effect* (with the Faraday magneto-optic effect for sensing), nuclear angular momentum effects, Coriolis force effects on various particles, and bulk fluid effects. The common thread running through these phenomena is that they are all based upon the inertial properties of matter at size levels ranging from nuclear or electronic to bulk. In the final analysis it is obvious that an inertial reference device must be based upon some inertial property of the material and therefore the heart of the understanding of the operation and potentialities of a particular phenomenon must lie in a knowledge of the inertial characteristics of the material. In the subsequent paragraphs in this chapter the nature of these phenomena mentioned above will be presented briefly with conclusions about the potential performance of devices based upon these phenomena. Later chapters will deal in more detail with the exposition of the phenomena and the analysis of their potential usefulness as inertial reference devices.

1. The Barnett-Faraday Effect

The work statement guiding the effort in this project specifically mentions the magneto-optic effect as one of the phenomena to be investigated. This effect, also known as the Faraday effect, is manifested by the rotation of the plane of polarization of a plane polarized beam of light when it passes through certain materials in the presence of a magnetic field. This effect is basically an interaction between the electromagnetic field of the incident beam and the motion of a charged particle in the presence of a steady magnetic field. In and of itself the Faraday effect does not have any inertial or motional dependence. However, when certain materials are given an angular rotation with respect to inertial space, there appears a proportional magnetization in the material. This effect is called the Barnett effect. Since the Barnett effect produces a net magnetization of the material, the Faraday effect is a possible mechanism for sensing this magnetization and consequently the angular rate of rotation of the device. It is this type of configuration that has been studied extensively here.

* A Barnett effect device with a Faraday effect sensor is termed a magneto-optical gyro.

level and signal-to-noise ratio for an earth's rate input. The various phenomena which were investigated include the Barnett effect* (with the Faraday magneto-optic effect for sensing), nuclear angular momentum effects, Coriolis force effects on various particles, and bulk fluid effects. The common thread running through these phenomena is that they are all based upon the inertial properties of matter at size levels ranging from nuclear or electronic to bulk. In the final analysis it is obvious that an inertial reference device must be based upon some inertial property of the material and therefore the heart of the understanding of the operation and potentialities of a particular phenomenon must lie in a knowledge of the inertial characteristics of the material. In the subsequent paragraphs in this chapter the nature of these phenomena mentioned above will be presented briefly with conclusions about the potential performance of devices based upon these phenomena. Later chapters will deal in more detail with the exposition of the phenomena and the analysis of their potential usefulness as inertial reference devices.

1. The Barnett-Faraday Effect

The work statement guiding the effort in this project specifically mentions the magneto-optic effect as one of the phenomena to be investigated. This effect, also known as the Faraday effect, is manifested by the rotation of the plane of polarization of a plane polarized beam of light when it passes through certain materials in the presence of a magnetic field. This effect is basically an interaction between the electromagnetic field of the incident beam and the motion of a charged particle in the presence of a steady magnetic field. In and of itself the Faraday effect does not have any inertial or motional dependence. However, when certain materials are given an angular rotation with respect to inertial space, there appears a proportional magnetization in the material. This effect is called the Barnett effect. Since the Barnett effect produces a net magnetization of the material, the Faraday effect is a possible mechanism for sensing this magnetization and consequently the angular rate of rotation of the device. It is this type of configuration that has been studied extensively here.

* A Barnett effect device with a Faraday effect sensor is termed a magneto-optical gyro.

The classical picture of the Barnett effect is as follows. Some atomic particle has an angular momentum J and a magnetic moment M which are proportional to one another:

$$M = \gamma J$$

When the lattice in which this atomic particle resides is rotated, a torque must be exerted on the atomic particle for it to maintain a physical orientation with respect to the lattice. This torque is produced by a small change in orientation of the particle with respect to its equilibrium position--the small change being in a direction tending to line up the particle angular momentum with the rotation axis. Before the rotation occurred, the magnetic momenta (and the angular momenta) of the particles were randomly distributed resulting in no net magnetization. During rotation all the particles tend to align their angular and magnetic momenta with the axis of rotation. This results in a component of magnetization along the axis of rotation. It can be shown that the relationship between the magnetic field and the angular rotation is one of proportionality, viz.

$$\vec{H}_{eq} = - \frac{1}{\gamma} \vec{\Omega}$$

where $\vec{\Omega}$ is the rate of angular rotation and $\vec{H}_{eq}$ is the magnetic field intensity that is equivalent to the rotation rate $\vec{\Omega}$ in terms of the effect on particle alignments. It further may be shown that γ, the gyromagnetic ratio, may be written as

$$\gamma = g \frac{e}{2m}$$

where

- e is the charge on the particle
- m is the mass of the particle
- g is the Lande g-factor which is of the order of unity

The Barnett effect is a phenomenon of electrons in orbit. Thus for electrons the value of $\frac{1}{\gamma}$ becomes

$$\frac{1}{\gamma} \sim \frac{1.14 \times 10^{-7}}{g} \quad \frac{\text{gauss}}{\text{rad/sec}}$$

From this an angular rotation rate of $\Omega = 10^{-4}$ rad/sec would be equivalent to a field of the order of 10^{-11} gauss. Therefore, to use the Barnett effect to detect angular rates (inertial) with a resolution of 10^{-4} rad/sec would require the measurement of a magnetic field with a resolution of 10^{-11} gauss.

The first problem that this poses is that of stray fields. If such a resolution is to be achieved it is obvious that all stray field must be reduced below this level. This is a formidable task. A survey of the literature indicates that under laboratory conditions, stray field may be reduced to about 10^{-6} gauss. Some work has also been done using superconducting metals as shields. There seems to be two problems here. First, a perfect superconductive cavity will trap and maintain whatever flux was within the cavity when it became superconducting. Consequently, in order to provide a cavity with stray flux lower than a specified amount, the cavity must be cooled to the superconducting state in a region free of flux to less than that specified amount. Secondly, superconducting materials have imperfections which would tend to pin whatever flux was contained within them to the cavity orientation. Thus rotation of the cavity would result in a like rotation of the trapped flux. There is one interesting possibility that has been presented recently. [16*] There are some indications that the flux trapped within a superconducting region is quantized. This implies that if a cavity is made superconducting in a region whose stray flux is below a certain level, the flux within the cavity after cooling will be identically zero. This effect is as yet too new to be evaluated properly.

If the Barnett effect is to be used as a means for sensing angular rotation some technique must be made to detect the very small resulting magnetic field. The Faraday effect--optical and microwave--was examined quite thoroughly for this role. This study included a search for materials having large Faraday effects, a study of the frequency dependence of the effects for possible resonant enhancement, and an analysis of potential magnetic field resolution attainable. Potential performance of an optical Faraday effect magnetic field measurement apparatus was evaluated in terms of a system composed of a light source, a polarizer, an active medium, an analyzer, and a photocell. The active medium was chosen to be tysonite since in a search of published data its Faraday rotation of about $6 \frac{\text{deg}}{\text{cm gauss}}$ was the largest found. An investigation of the optical frequency dependence of the Faraday effect was made to determine the

* Superscripts refer to numbered items in the Bibliography.

best frequency of operation. The investigation was based upon work reported in the literature and upon our own analyses. The conclusion was that operation near an optical resonance of the crystal did not result in larger rotations and introduced many problems such as absorption, frequency stability, etc. An analysis of the potential resolution of the system in measuring small magnetic field was made based upon an assumed minimum transmission of the analyzer and upon shot noise in the photo detector. The analysis indicates a minimum detectable magnetic field of the order of 10^{-8} gauss. This is a highly optimistic estimate. A similar analysis was made for a microwave Faraday effect device and here the minimum detectable field was of the order of 10^{-7} gauss.

These minimum detectable fields correspond to angular rates of 0.1 rad/sec and 1 rad/sec respectively. Thus an inertial rate reference based upon a Barnett-Faraday effect system would have a rate resolution several orders of magnitude larger than the earth's rate of rotation (10^{-4} rad/sec). This in conjunction with the problems of magnetic shielding mentioned above lead one to the conclusion that the Barnett effect is unlikely to yield a useful inertial reference instrument. A more detailed treatment of this material on the Barnett-Faraday effect system may be found in Volume I of this report entitled, "Theoretical Investigation of a Magneto-Optical Gyroscope," ESL-R-125 (I) — October, 1961.

2. Nuclear Angular Momentum Effects

In the preceding section it was seen that the Barnett effect is too small to be exploited usefully for inertial rate measurements. The magnitude of the Barnett effect depends directly upon the magnitude of

$$\frac{1}{\gamma} = \frac{2}{g} \frac{m}{e}$$

Since the mass-to-charge ratio $(\frac{m}{e})$ enters so prominently it was felt that the properties of nuclei whose $(\frac{m}{e})$ is of the order of 2000 times that of the electron merited investigation. Nuclei do not exhibit an effect like the Barnett effect of electrons. Nuclei tend to behave more nearly as free gyroscopes essentially decoupled from their surroundings; they tend to remain oriented in space. Nuclei, like electrons, however, possess a magnetic moment as well as angular momentum; the ratio again being expressed as a gyromagnetic ratio

$$\gamma = g \frac{e}{2m} = \frac{\Omega}{H}$$

There are two possible ways in which the nuclei may be utilized in an inertial reference device. Since they behave like free gyroscopes tending to maintain a fixed orientation in space, measurement of the direction of these magnetic gyroscopes with respect to the instrument axes would indicate the angular position of the instrument with respect to inertial space. The second method utilizes the fact that in the presence of an external d. c. magnetic field, the nuclei will tend to precess with respect to inertial space around the field at the Larmor frequency

$$\Omega = \gamma H$$

Thus measurement of precession frequency from an instrument that is rotating with respect to inertial space will result in a frequency which differs from the true Larmor frequency by an amount equal to the instrument angular rate. This latter principle is explored by the General Precision Laboratories[8] and therefore is not examined in detail in this study.

The system studied here uses the first principle mentioned above; namely, the free-gyroscope properties. The nuclei in a sample of matter are aligned by the application of a strong, external magnetic field. This field is then turned off. The nuclei now behave as microscopic free gyroscopes and maintain their orientation in space. Any angular motion of the instrument would result in a misalignment of the axis of the nuclei from the axis of the instrument. This misalignment being exactly equal to the angular rotation of the instrument. The magnetic aligning field is turned on causing the nuclei to undergo a damped precession around this external field until they are once again aligned. Pickup coils placed in the plane perpendicular to the aligning field will sense this precession and the magnitude of the voltage thus generated will be a function of the initial misalignment between the nuclei and the magnetic field. Thus, we have a measure of the net rotation of the instrument during the period the magnetic field was off. Operation under these conditions is intermittent since the device is not sensitive to motion during the readout and realignment and, furthermore, the device loses any information about what transpired in the previous motion sensitive interval.

An analysis of the performance of such a device has been made. This analysis was based upon operation as described above for the measurement of angular rates. In the analysis the effects of repetition frequency were included.

The objective of the analysis was to estimate the potential angular rate resolution of such a device. The first approach was on the basis of the limitations imposed by amplifier noise in the readout system. For a given angular misalignment between the nuclear magnetization and the device magnetic field direction (the misalignment caused by rotation of the apparatus), the change in magnetic energy of the nuclei can be calculated. It is assumed that this is the maximum available signal energy which must be sensed by the readout coil and amplifier to determine the angular change. The readout coil and amplifier, however, add a certain amount of noise energy to the signal energy thus imposing a minimum resolvable angular change. Using representative numbers for this system it is estimated that an optimistic minimum detectable rate would be of the order of 10^{-2} rad/sec (about 100 times earth's rate) which is not considered very attractive.

A second analysis of the minimum detectable angular rate was made based upon a suggestion by Culver.[3] This analysis is more fundamental than the previous one. The basis of the analysis is as follows. The external magnetic field causes the nuclear spins to line up either parallel or antiparallel to the field. The relative numbers are determined by a random process having a Boltzmann temperature distribution. After the apparatus has moved it is desired to determine the component of the original magnetization along the new apparatus direction. Since the original orientation of the particles is a random process, so too is the component along a new axis. Consequently, the determination of the component involves finding the average of a random variable from a finite number of samples (nuclei). The average thus found is not equal to the true average but rather approaches the true average as the number of samples increases. The relation between such an average and the true average (infinite samples) can be calculated. This has been carried out for the system described above. For typical numbers, including a sample of approximately 10^{24} nuclei, the minimum detectable angular rate turns out to be about 10^{-7} rad/sec (which is roughly 10^{-3} earth's rates). The 10^{24} nuclei is the number of active nuclei and is equal to the number of nuclei in a gram-molecular weight of the substance. The 10^{24} nuclei, if of water, would require 16 cc of water if all nuclei were active. This analysis is more optimistic than the previous one and also more fundamental. This more fundamental limit may also

be significantly more difficult to reach than the previous limit.

The conclusion reached here is that angular rate measurement devices based upon utilization of the gyroscopic properties of nuclear particles do not offer sufficiently high potential performance to warrant prolonged development.

A possible exception to this general conclusion may exist in the case of nuclear gyros based on precise measurements of Larmor frequencies. The microwave pumping technique (RASER effect)[10, 11] makes possible a narrowing of the line width of the nuclear magnetic resonance effect by an order of magnitude or more. However, a nuclear precession approach still seems questionable in view of disparity between the precessional frequencies (even in weak magnetic fields these are in the 10 to 100 kilocycle per second range) and the angular rates to be measured (in the fractional earth's rate range).

A more detailed description and analysis of systems based upon nuclear effects may be found in Chapter II of this report.

3. Coriolis Force Effects with Small Particles

In the preceding sections, the exploration of physical phenomena for possible application to inertial reference devices centered on the angular motion properties of atomic particles. Particles with linear momentum also offer inertial properties which might be exploited to sense inertial angular motion. Forces of the type described here are called Coriolis forces. Possible devices utilizing this force will be examined in this section.

As is well known, if a particle has a linear momentum in a particular direction, a force is required to change this direction. In particular, if the particle is given a linear momentum $\bar{p}$ with respect to a coordinate system fixed on some apparatus which is rotating with an angular velocity $\bar{\Omega}$, then the particle must be subjected to a force $-\bar{F}_c$ --the negative of Coriolis force--if it is to maintain its position with respect to the apparatus. The Coriolis force is given by

$$\bar{F}_c = -2\ \bar{\Omega} \times \bar{p}$$

where the angular velocity $\bar{\Omega}$ is that of the apparatus with respect to inertial space and the momentum $\bar{p}$ is measured with respect to the apparatus reference frame. Accordingly, devices to sense angular rates with respect to inertial coordinates can be based upon the measurement of Coriolis forces.

A number of configurations using this principle for the measurement of inertial angular rates have been studied. These have been analyzed for the magnitude of the output effect for angular rates corresponding to the earth's rate of rotation. In general, detailed noise analyses were not carried out; rather, engineering experience was used to evaluate the possibility of sensing effects of the calculated magnitude.

The first system examined utilized a dumb-bell shaped rigid atomic-size particle having an electric dipole moment; a number of such particles are assumed to be embedded in a lattice structure. The lattice structure provides "spring" restoring forces that tend to keep the particle fixed in relation to the lattice. An alternating electric drive field along one axis interacts with the dipole moment causing the particle to oscillate about its mean position. Thus it acquires a periodic velocity in the direction of the applied field. Rotation of the lattice about an axis normal to the applied field direction will result in a periodic torque on the particle in the third orthogonal direction. This torque is caused by the Coriolis forces. Since the particle has a dipole moment, this latter oscillation produces an oscillating polarization along this axis which may be sensed to measure the angular rate of rotation. The magnitude of the polarization is, however, very small; typical numbers give a polarization magnitude of the order of 10^{-15} volts/meter for an angular rate of the order of earth's rate. It is fairly obvious that measurement of voltages of this magnitude is impractical. The principle factor making the effect so small is the large lattice forces which hold the particle rigidly in place.

In an effort to attain larger effects, free particles such as in liquids and gases were examined. In this case, an elastic-restraint type of effect is produced by thermal agitation which tends to cause the dipoles to have a uniform, random orientation. An alternating electric drive field will cause the dipoles to oscillate about their mean position (as established by the thermal equilibrium) thus achieving the desired velocity in the direction of the drive field. With rotation of the apparatus, there is an oscillation in the orthogonal direction as in the previous case. An analysis was made using a Maxwell-Boltzmann distribution to approximate the thermal distribution. Typical numerical values give a polarization of approximately 10^{-10} volts/meter for earth's rate. This is, indeed, larger than the previous case but still impractically small.

In both the Coriolis force cases examined thus far, the magnitude of the effect depends directly upon the particle size. The atomic size particles considered resulted in atomic size effects. Colloidal particles, on the other hand, have diameters ranging from 0.01 microns to 10 microns and thus span the size gap between atomic and macroscopic size. Because of their large size compared to the atomic size particles, colloidal particles were investigated for possible utility in Coriolis force type angular rate sensing devices.

The fundamentals of colloidal particle suspensions are not well understood. It is generally agreed that the particles have electric charge adhering to their surfaces and this electric charge plays an important role in maintaining the particles in suspension. The type of configuration studied is as follows. The charged particles are given a velocity by an applied magnetic field. If the suspension container is given an angular velocity about an orthogonal axis, the particles will experience a Coriolis-like force in the remaining orthogonal direction. This force will result in a disturbance of the equilibrium distribution of particles and thereby give rise to an electric field in the direction of the force. This electric field, of course, is the electrical indication of the angular rate of the apparatus. Some typical numbers in a brief analysis show an output field of about 10^{-7} volts/meter for one earth's rate. Again this seems impractically small.

The general conclusion of this study of Coriolis force effects using small particles seems to be that the Coriolis effects are too small compared to the other, much larger, forces seen by the particles. As a result the observable effects are quite small--so small as to seem, in the light of our present engineering experience, as to be unmeasurable. A more detailed discussion may be found in Chapter III.

4. Bulk Fluid Effects

As a supplement to the study of atomic particles for possible inertial reference properties, the properties of fluids and superfluids were investigated. In a fluid, disturbances are propagated by a wave mechanism which, in the case of shear disturbances, depends upon the viscosity of the fluid. Therefore, a fluid in a spherical container is coupled to motion of the container only through the fluid viscosity. If there is no viscosity, there is no coupling and the fluid remains fixed in inertial space. Reports of the unusual superfluid properties

of liquid helium II suggested an investigation along these lines.

An analysis was made of the motion of a fluid between two infinite flat plates and in an infinite cylinder in response to motion of the walls. The solutions show a wave-like propagation of the motion to the interior of the fluid with time constants determined largely by the kinematic viscosity. With this analysis in hand the viscous properties of liquid helium II and other more common fluids were investigated. The properties and behavior of helium II are neither well understood nor well known. However, it is known that the property of zero viscosity of this liquid that is needed for decoupling exists only in thin films of the fluid. Furthermore, this property depends upon the motional state of the fluid. As a consequence, there is no reason to prefer helium II to normal helium for this application. The kinematic viscosity of normal liquid helium is lower than that of any other known substance. However, this kinematic viscosity is only an order of magnitude below that of mercury and therefore does not seem to offer exceptional promise over what might be accomplished with more common fluids.

For a step change in angular position of the container, the inner layers of the fluid respond with a characteristic transient change in position. The position each layer, in the absence of turbulence, asymptotically approaches is the final position of the container. The effective time constant of this motion for mercury is of the order of 2000 seconds. Thus after long periods the fluid loses memory of its original orientation but over short periods the interior fluid remains fixed in space.

The utilization of fluid properties in inertial reference devices has been examined from the points of view of both angular rate and angular position devices. The response of an interior layer of liquid to a suddenly applied constant angular velocity of the container is a transient terminating in a constant lag in the position of the fluid with respect to the container. This asymptotic lag is proportional to the case velocity and thus could serve as a measure of angular rate. The response time, however, in the case of mercury, is 2000 seconds. This means the asymptotic lag is not useful for rate sensing in most applications.

In a position sensing device, use is made of the fact that the interior portion of the liquid does not respond appreciably to the case motion during

times short compared to this time constant. If the sensing unit is mounted on a platform and the platform is driven by a servomotor actuated by the instantaneous fluid lag angle relative to the container, it is possible to achieve stabilization of the platform with respect to inertial space. With this method stabilization is obtained for periods that may be arbitrarily long relative to the sensing unit time constant. The discussion thus far of possible techniques to exploit the visco-inertial properties of fluids in inertial reference devices has tacitly assumed that it is possible to sense the position of the fluid with respect to the container. In general the performance of the device will be limited by the resolution with which this angle can be measured as well as by the fluid properties as described above. A preliminary analysis of the requirements that must be met by the fluid position sensor has been made. The problem of realizing such a sensor has received only limited attention.

The basic conclusion from the above study of bulk fluid devices is that an ordinary fluid such as mercury is sufficiently decoupled from its container so as to provide an acceptable inertial reference for platform stabilization providing the fluid position sensing problem can be solved. Because a spherical form of instrument could be made sensitive to motions about three axes, this approach may have advantage over conventional gyroscopes. Therefore a continuation of this investigation is desirable and in particular the fluid position sensing study should be carried further.

Supporting information for the conclusions of this section can be found in Chapter IV.

C. CONCLUSIONS

The investigation reported here has as its objective a broad examination of fundamental physical phenomena from the viewpoint of their utilization in devices for sensing angular positions or rates with respect to inertial coordinates. Such devices should have some promise of ultimately becoming competitive with present mechanical gyroscopes by offering advantages in reliability, simplicity, or performance in order to merit serious development. From a research management point of view it is important to assess the potential performance offered by a number of "exotic" phenomena before embarking upon costly research programs aimed at exploiting particular ones.

It is quite evident in searching for properties or phenomena that might be useful in inertial reference devices that the only properties of particles or matter that are applicable are inertial properties. Only those properties which must be described with respect to an inertial reference system can offer any utility in an inertial reference device. While this may be a painfully obvious truism, it is nonetheless worth stating since it is a common thread running through the phenomena and systems studied.

The phenomena studied as possible bases for inertial reference systems are: (1) the magneto-optical gyro based on the Barnett-Faraday effect; (2) free nuclear angular momentum effects; (3) Coriolis force effects in atomic and colloidal particles; and (4) visco-inertia effects in bulk fluids. For each of the four classes of phenomena, the effects are dependent upon the translational or rotational inertia of the element. The Barnett effect is a manifestation of the angular momentum of orbital electrons. Also, with the nuclear particles it is their angular momentum that may be exploitable. The Coriolis force is basically a translational momentum effect and in the bulk fluid it is simply the mass and low viscosity that was to be utilized. Thus the investigation has touched upon all of the commonly considered inertial properties of particles.

The evaluation of the potential performance of devices based upon these effects was made by studying a representative configuration using the effect and trying to estimate performance limitations. Sensitivity of the device to angular rates less than the rate of rotation of the earth ($\sim 10^{-4}$ rad/sec) was considered necessary for the device to warrant serious further development. As indicated above, some of the analyses included a study of noise limitations while in other cases the performance was judged on the basis of engineering experience.

Behind these analyses, there were other, perhaps more fundamental, limitations which were considered. One such approach is described as follows. The principle of operation of one device, the magneto-optical gyro, is based on the Barnett and Faraday effects in a crystal. Such a solid-state angular motion sensor must depend upon the change in properties of the solid when it is caused to rotate. Those differences, as indicated above, must be caused by inertial or gravitational forces on the various particles that make up

the solid. From the two dimensional equations of motion for a particle in polar coordinates, the radial and tangential forces on it are

$$F_r = m\ddot{r} - m(r\dot{\theta}^2) \tag{1.1}$$

$$F_\theta = mr\ddot{\theta} + 2m\dot{r}\dot{\theta} \tag{1.2}$$

From these the changes in the forces needed to balance a small angular rate of rotation Ω of the apparatus are

$$\Delta F_r = -2mv_\theta\Omega \tag{1.3}$$

$$\Delta F_\theta = 2mv_r\Omega \tag{1.4}$$

Note that the changes in these inertial forces are both of the same form. In order to relate these forces to familiar effects whose measurability can be estimated from our experience, we can compare these forces to those caused by magnetic and electric fields. For magnetic fields, the force on a charged particle moving with velocity v is

$$F_H = q\bar{v} \times \bar{B} \tag{1.5}$$

The magnetic field B_{eq} that produces a force on the particle equivalent to the force changes caused by the angular rate of the apparatus is

$$B_{eq} = \frac{2m}{q}\Omega \tag{1.6}$$

This follows from Eqs. 1.3 and 1.4 in combination with Eq. 1.5. Thus we see that a magnetic field is equivalent to an angular rate in terms of the resultant forces acting on a charged particle. A similar relation holds for electric fields

$$E_{eq} = \frac{2m}{q}\Omega \tag{1.7}$$

Next we may calculate the fields equivalent to one earth's rate of rotation to get an estimate of the measurement problem. The equivalent field for various particles is as follows

Table I

Fields Equivalent to One Earth's Rate of Rotation

Particle	q/2mc (cgs)	B_{eq}(gauss)	E_{eq}(v/cm)
Electron	10^{7}	7×10^{-12}	2×10^{-9}
Proton	5×10^{3}	1.4×10^{-8}	4×10^{-6}
Ion of 200 proton mass	25	3×10^{-6}	9×10^{-4}

Now, present solid state experiments are hard pressed to measure effects due to magnetic fields of less than 10^{-3} gauss. Therefore, it is evident from the table that the measurement of effects in solid-state devices caused by angular rates that give rise to forces equivalent to such low magnetic fields is probably impossible using present techniques.

A further related problem is that of shielding. In any such device it is obvious that magnetic shield must be provided to reduce the stray magnetic field below the equivalent field of the effect being measured. Shielding to maintain magnetic fields constant to better than approximately 10^{-6} gauss is beyond today's state of the art. Thus simple electron and proton based gyros are deemed impractical because of the magnetic shielding problem.

Another fundamental limitation arises from the limited sample size available in any practical device. A measurement involving fundamental particles is basically an average over a number of particles of a random variable. With only a finite number of samples (particles) from which to determine the average value, there is uncertainty in its determination. This is quite fundamental and not amenable to improvement by more sophisticated experimental techniques. With this criterion applied to the nuclear precession sensor, a gram molecular weight of the active nuclear material would give a precision limit of the order of 10^{-7} rad/sec or 10^{-3} earth's rate as an absolute lower bound. If this precision could be obtained with a relatively simple piece of apparatus it would be worth striving for. However, a nuclear magnetic gyro promises to be quite a complex device so it is questionable if it is worth the effort except as a research goal.

On the basis of the foregoing, it was decided that angular momentum effects at the atomic level were not large enough to form the basis of an angular motion sensor. As a result, other effects were examined. These were Coriolis forces at atomic and colloidal levels and bulk fluid inertial effects. At the atomic level, systems based upon lattice-bound particles and upon free particles were examined. In the case of the bound particle, the lattice forces are the restraints; for free particles it is the "thermal" forces that play this role. In both cases the restraining forces are so much larger than the Coriolis forces that measurement of angular movement by these means is infeasible. At this point, colloidal particles were examined to see whether these larger particles might offer larger, more measurable effects. From an electric effects point of view, not very much is known about the statics or dynamics of colloidal suspensions. In spite of this, a brief analysis indicated that here, too, the observable effects are small and probably easily masked by other unrelated effects. A brief excursion was made into inertial effects in bulk fluids. This excursion was made in the hope that the superfluid properties of liquid helium II might be exploited. These properties do not exist except under conditions that cannot be met in an angular motion sensor. The inertia-viscous coupling ratio for normal liquid helium was only of the order of 10 times better than that of mercury. The investigation showed that a motion sensor based upon fluid inertia properties theoretically could serve as a sensor for a stable platform. The problem of measuring the displacement of an inner shell of the fluid relative to the container remains to be solved.

In summary, as the result of this investigation, there appears to be no obvious way of using microscopic and colloidal phenomena as alternatives to mechanical gyroscopes. We have examined electronic, nuclear, molecular, colloidal, and bulk fluid effects. None of the approaches that we have investigated appear to be sufficiently promising to justify large-scale programs aimed at the development of practical angular motion sensors. However, in spite of the rather remote prospect of finding a practical way of building a useful gyroscope based on microscopic phenomena, a limited amount of basic research in certain areas related to

this objective could be worthwhile. Included among these areas should be studies of magnetic shielding and nuclear magnetic masers (rasers) to mention just two. The justification of this research should be the expected increase of specialized knowledge in these fields rather than the hope of finding a practical gyroscope based on microscopic phenomena.

CHAPTER II

NUCLEAR ANGULAR MOMENTUM SENSOR

A. INTRODUCTION

Atomic nuclei and nuclear particles may have an intrinsic "angular momentum" which causes them to behave similar to a classical spinning gyroscope. If in addition they have magnetic moments then it is possible to orient the particles with an external magnetic field, and to sense magnetically their orientation or their motion. This coupling between angular momentum and magnetic field suggests the possibility of constructing a "gyroscope" without moving parts, and has inspired the investigation, by several research organizations, of the application of nuclear magnetic resonance phenomena to angular motion measurement.[8]

Two general categories of nuclear particle gyroscopes will be discussed in this report. The first is a "free gyro", in which the nuclear spins within a sample are first aligned by a magnetic field within the instrument, and then allowed to "drift" in a field-free region, where the total magnetization retains its initial orientation in inertial space due to the gyroscope-like behavior of the nuclear spins. After a period of time the remaining total nuclear magnetization is measured, and the angle between this magnetization and the magnetic field with which the nuclei were originally aligned indicates the angle through which the instrument turned during the "drift" period. The nuclear magnets can then be realigned with the instrument-fixed bias field again to repeat the process.

The second type of nuclear gyro that will be treated is the "inertial frequency measuring" type. In this instrument the nuclear magnets are forced to precess around a constant bias field by an RF magnetic field generated within the instrument. A detectable resonance occurs when the RF field is revolving at a rate corresponding

to the Larmor precession frequency for the constant bias field strength used, and the frequency of the revolving field would be set at or near the center of this resonance. If the instrument is rotated mechanically about the bias field axis, the rate at which the nuclear magnets see the RF field revolve becomes faster, or slower by the frequency of mechanical rotation, and sensing equipment rotating with the instrument would observe a departure from resonance. This might be observed and converted into an indication of angular rate in several ways, some of which are described in Section C.

B. NUCLEAR FREE GYRO

If the nuclear particles within a sample are aligned by a large external magnetic field and then kept in a field-free container, the direction of the total magnetization will remain the same in inertial space regardless of the motion of the container. (The magnitude of this total magnetization will decay with time, however.) It is then possible in principle to look into the container at intervals and determine the current direction of the nuclear magnetization, thus obtaining a simple inertial reference.

In practice it is necessary to extract some energy from the collection of nuclear particles each time such a measurement is made, the exact amount of energy needed depending on the effective noise level at the sensor input and on the accuracy desired. Because of the very small amount of magnetic energy that can be stored in the nuclear magnetic moments of a reasonable volume of material, it would probably not be possible to interrogate a sample of nuclei more than a few times before realigning them. Since it would probably be desirable to sample the nuclear magnetization several times a second, it appears necessary to realign the nuclear magnetization between sampling times.

A typical configuration might consist of a nuclear sample container surrounded by a biasing coil capable of generating a relatively large (e.g., 1000 gauss) field for aligning the nuclei, and some means

of sensing the direction of the nuclear magnetization. The bias coil would be switched on briefly to align the nuclei, and then shut off. After a period of time the residual nuclear magnetization is measured, and the angle measured between the direction of the remaining magnetization and the bias field axis is the angle through which the instrument rotated during the time the bias field was off. Then the bias field is turned on again, and the cycle repeated.

One way of measuring this angle between bias field axis and residual magnetization depends on the transient effects which occur while the nuclear particles are being realigned with the bias field axis. During this realignment period, the component of the residual magnetization perpendicular to the bias field axis precesses around the bias field axis and would therefore induce a voltage in a sensing coil orthogonal to the biasing coil. The voltage induced is proportional to the magnitude of the perpendicular component of magnetization, which in turn is proportional to the sine of the angle through which the instrument rotated during the period between bias pulses. Consequently this sensing scheme provides an indication of the instrument's rate of rotation. The magnitude of voltage induced in the sensing coil per unit angular rate can be estimated as a function of the magnetic characteristics of the sample nuclei. With this, the minimum detectable rate could be estimated based on assumed values for the electrical parameters of the instrument and assumed noise levels in the system. However, a simpler and perhaps more fundamental estimate of the performance limitations will be made which depends less upon the detailed structure of the instrument. This estimate is based upon the maximum magnetic energy available for sensing the rotation.

The residual nuclear magnetization, M_o, remaining at the start of a bias field pulse is determined by the bias field magnitude H_b, the nuclear susceptibility X_o, the longitudinal relaxation time T_1, and the periods during which the bias field is turned on (t_p) and off (t_d). M_o can be found by assuming an exponential growth and

decay of the magnetization during the polarizing and drift periods, with time constant T_1, and solving for the steady-state value:

$$M_o = X_o H_b \frac{1-e^{-\frac{t_p}{T_1}} e^{-\frac{t_d}{T_2}}}{1-e^{-\left(\frac{t_p}{T_1}+\frac{t_d}{T_2}\right)}} \tag{2.1}$$

During the polarizing period the magnetization grows with time constant T_1, and during the decay period, in the absence of external fields, it decays with time constant T_2. The angle through which the magnetization rotates during the time H_b is off is

$$\theta = \Omega t_d \tag{2.2}$$

The magnetic potential energy of a dipole of moment M directed at an angle θ to a magnetic field H is

$$W_M = - MH \cos\theta \tag{2.3}$$

When the bias field is turned on the residual magnetization of the nuclear sample initially makes an angle θ with the bias field. The decrease in magnetic potential energy which accompanies its realignment with the bias field is

$$\Delta W_M = M_o H_b (1 - \cos\theta) V \tag{2.4}$$

where V is the volume occupied by the nuclear sample. Substituting expressions 2.1 and 2.2 for M_o and θ gives the decrease in magnetic potential energy:

$$\Delta W_m = X_o H_b^2 V (1-\cos\Omega t_d) \frac{\left(1-e^{-\frac{t_p}{T_1}}\right)e^{-\frac{t_d}{T_2}}}{1-e^{-\left(\frac{t_p}{T_1}+\frac{t_d}{T_2}\right)}} \tag{2.5}$$

If $(\frac{t_p}{T_1} + \frac{t_d}{T_2}) << 1$, then the exponentials can be approximated by the first two terms of their power series:

$$\Delta W_M = X_o H_b^2 V (1-\cos \Omega t_d) \frac{t_p (T_2 - t_d)}{t_p T_2 + t_d T_1} \qquad (2.6)$$

The fraction $\frac{t_p(T_2 - t_d)}{t_p T_2 + t_d T_1}$ appearing in Eq. 2.6 is always less than unity, and increases with increasing T_2. In order to get the greatest ΔW_M it would therefore be desirable to choose a material with a long T_2. However $T_2 \leq T_1$, so the ideal case can be represented by setting $T_2 = T_1$:

$$\Delta W_M = X_o H_b^2 V (1-\cos \Omega t_d) \frac{t_p (T_1 - t_d)}{T_1 (t_p + t_d)} \qquad (2.7)$$

Neglecting t_d with respect to T_1, and defining $\frac{1}{t_p + t_d} = f_s$ = sampling frequency:

$$\Delta W_M = X_o H_b^2 V f_s t_p (1-\cos \Omega t_d) \qquad (2.8)$$

For small angles Ωt_d, $\cos \Omega t_d \approx 1 - \frac{1}{2} \Omega^2 t_d^2$ so

$$\Delta W_M = \frac{1}{2} \Omega^2 X_o H_b^2 V f_s t_p t_d^2 \qquad (2.9)$$

In practice the sampling rate f_s would be determined by system bandwidth or response time requirements. Assuming that f_s if held fixed, then, t_p and t_d should be chosen so that the largest change in magnetic potential energy ΔW_M is obtained with $t_p + t_d = \frac{1}{f_s}$ held constant. This leads to the choice of

$$t_p = \frac{1}{3f_s}$$

$$t_d = \frac{2}{3f_s} \qquad (2.10)$$

So the largest ΔW_M is

$$\Delta W_M \leq \frac{2\Omega^2 X_o H_b^2 V}{27 f_s^2} \qquad (2.11)$$

Each time the bias field is pulsed, an amount of energy equal to the ΔW_M of Eq. 2.11 is released as the nuclear moments are realigned with the bias field, provided that the bias field is kept on until the reorientation has been completed. Each magnetic dipole releases its change in magnetic potential energy as RF energy at frequency $\omega_{rf} = \gamma H_{loc}$, where H_{loc} is the magnetic field intensity at the location of the dipole. Inhomogeneities of the biasing field, radiation damping from currents induced in the sensing coil and the magnetic fields generated by the nuclear particles themselves combine to produce a variation in H_{loc}, and consequently in ω_{rf}, over the volume of the sample. Consequently, the radiation from the collection of particles, initially in phase, becomes more and more incoherent as time passes, due to the spread in their precession frequencies. The length of time for which the radiation is essentially coherent is the effective transverse relaxation time, T_2^*. The amount of energy available to the detector in the form of coherent radiation is therefore necessarily less than the decrease in magnetic potential energy of Eq. 2.11. The total energy available to the detector per bias field pulse is also decreased by the amount of the transmission losses. For these two reasons the amount of RF energy W_{rf} which reaches the detector per bias field pulse is necessarily less than the change in magnetic potential energy ΔW_M of Eq. 2.11, the exact difference being determined by the detailed construction of the instrument and the characteristics of the

nuclear magnets. The maximum amount of energy available to the detector during each pulse of the bias field is therefore

$$\omega_{rf} \leq \Delta W_M = \frac{2\Omega^2 X_o H_b^2 V}{27 f_s^2} \qquad (2.12)$$

It is next necessary to decide on a suitable criterion of "successful" detection of the signal, so that the minimum detectable value of ω_{rf}, and hence of Ω, can be estimated. The detection of a given recurring waveform in the presence of white Gaussian noise can be treated by the methods of decision theory. If it is assumed for the moment that the probability of occurrence of the signal during a particular decision interval (i. e. the probability that the instrument has been rotated during the decision interval) is independent of the occurrence of a signal during previous decision intervals then the type of detector which produces the highest probability of detection for a given false alarm rate is a matched filter followed by a threshold detector, where the threshold is adjusted so that the average frequency at which input noise alone causes an output from the filter which exceeds the threshold is not greater than the desired maximum false alarm rate. If the longest allowable time interval between observations of Ω is τ seconds, one sample of the signal would contain about τf_s pulses, each of energy ω_{rf}, for a total signal energy per decision interval

$$E = \frac{2}{27} \Omega^2 X_o H_b^2 V \left(\frac{\tau}{f_s}\right) \qquad (2.13)$$

Under the assumptions listed above, the probability of detecting the signal, for a specified maximum false alarm rate, is determined by the ratio of signal energy per decision interval to noise power per cycle per second. For a false alarm rate of about one in fifteen sampling intervals, a detection probability of 50 % is obtained for a ratio[1]

$$\frac{E}{N_o} = 4 \tag{2.14}$$

where N_o is the equivalent input noise power per cps. For this definition of "minimum detectable signal," Eq. 2.13 gives the minimum detectable mechanical angular rate as

$$\Omega^2_{min} = \frac{54\ N_o\ f_s}{X_o\ H_b^2\ V\tau} \tag{2.15}$$

By further signal processing beyond the fiter and detector assumed here the minimum detectable rate might be decreased slightly below that indicated in Eq. 2.15 since successive samples of the signal are not truly independent. However, the improvement would be small, and probably more than compensated by the assumption of Eq. 2.12.

To estimate the numerical value of expression 2.15 for practical parameter values, it is necessary to see what materials have the highest nuclear magnetic susceptbility X_o. For materials and temperatures where the Curie law is applicable, the static nuclear magnetic susceptibility is

$$X_o = \frac{n\ N_a\ \rho\ I\ (I+1)\ \gamma^2 \hbar^2}{3\ K\ T\ M} \tag{2.16}$$

where

- n = Number of desired type of particles per molecule
- N_a = Avogadro's number = 6×10^{23}
- ρ = density of material
- I = spin quantum number of desired particle
- γ = gyromagnetic ratio of particle
- $\hbar$ = 1.05×10^{-27} erg-seconds
- k = 1.38×10^{-16} ergs per degree Kelvin
- T = temperature, degrees Kelvin
- M = Molecular weight of material

The assumption that $T_2 \approx T_1$ in Eq. 2.7 leading to a large average magnetization excludes most solids, for which $T_2 << T_1$. It is apparently desirable to operate the device at a low temperature as indicated in Eq. 2.16 so a material should be selected which remains liquid at cryogenic temperatures. Also, protons have one of the higher gyromagnetic ratios, so it appears liquid hydrogen would be a good material. For liquid hydrogen at $20^{\circ}K$, $X_o = 3 \times 10^{-9}$ ergs/gauss^2/cm^3. Since it has been assumed in calculating X_o that the nuclear sample would be refrigerated to $20^{\circ}K$, then the thermal noise generated in the pickup coil will be very small and the equivalent noise input power per cps, N_o, will be almost entirely due to detector (amplifier) noise. The RF signal frequency is around a megacycle for large pulsed bias fields and the quietest amplifiers in this range are probably low-noise triodes, which have input noise powers of around 3×10^{-18} watts per cps.[2] Using these figures for N_o and X_o and assuming V = 30 cm^3 and H_b = 200 gauss, the minimum detectable angular rate is

$$\Omega^2_{min} = \frac{1}{2} \times 10^{-6} \left(\frac{f_s}{\tau}\right) \text{ radians}^2/\text{sec}^2 \qquad (2.17)$$

The pulse frequency f_s and system dominant time constant are related by $f_s \gtrsim \frac{2}{\tau}$ so, in terms of desired time constant τ,

$$\Omega^2_{min} = 10^{-6} \left(\frac{1}{\tau}\right)^2 \text{ radians}^2/\text{sec}^2 \qquad (2.18)$$

This is thought to be an optimistic estimate. Somewhat larger X's might be obtained by operating at lower temperatures with other materials, but the improvement would probably not be great. Certainly, not more than a factor of 10.

A more fundamental limitation on the performance of nuclear gyroscopes has been pointed out by Dr. W. H. Culver of the Rand Corporation.[3] His analysis can be applied to this particular type of instrument as follows.

The biasing field establishes a particular set of directions in which the nuclear particles can be aligned. In the case of protons, as has been assumed for this analysis, the particles can be aligned either with their dipole moments in the direction of the bias field or exactly opposite to the bias field. Let the probability that a dipole is oriented in the direction of the bias field be η, so that the probability of the opposite orientation is $(1-\eta)$. If the sample contains N dipoles, each of magnetic moment μ, then the net magnetization measured in the bias field direction, say the z-axis, is

$$M_Z' = N\mu(2\eta-1) \tag{2.19}$$

If the magnetization component is measured along an axis Z' which makes an angle α with the bias field axis, then the magnetization component along this axis is

$$M_Z' = N\mu(2\eta-1)\cos\alpha \tag{2.19a}$$

The same magnetization component, M_Z', could have been obtained if all of the dipoles were aligned parallel and antiparallel with the Z'-axis, with probabilities η' and $(1-\eta')$, respectively provided η' and η are related by

$$M_Z' = N\mu(2\eta'-1) = N\mu(2\eta-1)\cos\alpha, \text{ or}$$

$$\eta' = \frac{1}{2} + \frac{1}{2}(2\eta-1)\cos\alpha \tag{2.20}$$

The Z and Z'-directions, separated by the angle α can be associated with the directions along which the protons are initially oriented (Z) and along which their magnetization is later sensed (Z'). If the instrument is not rotated between the time the nuclei are aligned and the time their orientation is sensed, then α is the mechanical angle between aligning coil axis and the sensitive axis of the sensor. If the

instrument is rotated mechanically before the measurement along Z' is made, then the effect is to increase or decrease α by an amount Ωt_d. This causes a change in η', which is, for small angles Ωt_d,

$$|\Delta \eta'| = \frac{1}{2} \Omega t_d (2\eta - 1) \sin \alpha \qquad (2.21)$$

The change in the number of protons with their dipole moment projecting in the positive direction along the Z' axis would be

$$|\Delta N| = \frac{1}{2} \Omega t_d N (2\eta - 1) \sin \alpha$$

To detect the largest change ΔN for a given Ω, it is apparently desirable to choose $\alpha = 90^\circ$. This means the sensing and biasing axes are perpendicular as was assumed to be the case in the earlier analysis of the instrument under consideration. Then the change in the number of protons with dipole moments projecting along the +Z' axis would be

$$|\Delta N| = \frac{1}{2} \Omega t_d N (2\eta - 1) \qquad (2.22)$$

The problem of detecting an angular rate is therefore equivalent to measuring the change ΔN in the number of protons oriented in the + Z' direction. The simplest way to make this measurement, ultimately, would be to remove the protons individually from the sample and count those with projections in the positive-and negative -Z' directions. There are two sources of experimental error in this sort of hypothetical measurement. First, even if a single proton could be isolated, there would be a large error involved in determining the projection of its very weak magnetic moment in a given direction. This sort of realistic limit to the accuracy of the instrumentation was considered in the previous analysis. However, there is an additional source of error due to the fact that even if a perfectly noiseless measurement of the dipole projection of each

proton were possible, there would still be a statistical uncertainty in inferring the true change in η' and hence in Ω from a measurement of ΔN on a finite number of particles.

The standard deviation of repeated measurements of the number of protons with dipole moments projecting in the positive Z' direction, for the same value of η', is given in reference 3 as

$$\sigma_N = \sqrt{N\eta'(1-\eta')} \tag{2.23}$$

The criterion used in Eq. 2.14 to estimate minimum detectable angular rate is approximately equivalent to $\Delta N = 2\sigma_N$, or from Eqs. 2.22 and 2.23, the minimum detectable rate would be

$$\Omega_{min} = \frac{4\sqrt{\eta'(1-\eta')}}{t_d(2\eta-1)\sqrt{N}}$$

Since $\eta' \approx 1-\eta' \approx \frac{1}{2}$, and the best sensor signal-to-noise ratio was found to occur for $t_d = \frac{2}{3f_s}$ (Eq. 10), then

$$\Omega_{min} = \frac{3}{f_s(2\eta-1)\sqrt{N}}$$

The probability η can be determined from the magnetic energy level splitting and the temperature of the sample, assuming a Boltzmann distribution. This gives

$$(2\eta-1) = 10^{-7}\left(\frac{H}{T}\right)$$

where T is the sample temperature in degrees Kelvin and H is the equivalent magnetic field in gauss which would produce the amount of magnetization existing at the time the nuclear particles are interrogated. From Eq. 2.1, this field is equal to

$$H = H_B \frac{(1-e^{-\frac{t_p}{T_1}})\, e^{-\frac{t_d}{T_2}}}{1-e^{-(\frac{t_p}{T_1}+\frac{t_d}{T_2})}}$$

If the earlier assumptions that $T_2 = T_1$, $t_p + t_d << T_1$, and $t_d = \frac{2}{3f_s}$ and $t_p = \frac{1}{3f_s}$ are again made, then $H = \frac{1}{3} H_B$. The minimum detectable rate would then become

$$\Omega_{min} = \frac{9 \times 10^7 \, T}{f_s \, H_B \sqrt{N}} \qquad (2.24)$$

For the previous assumptions of $T = 20^{\circ}K$, $H_B = 1000$ gauss, $f_s = 10$ cps, and assuming $N = 6 \times 10^{23}$ protons, the "statistical" uncertainty limit is

$$\Omega_{min} = 2 \times 10^{-7} \text{ radians/second.}$$

The "statistical uncertainty" limit to the accuracy of an NMR gyro as estimated here is considerably better than the limit estimated on the basis of electronic noise levels. This indicates considerable margin for improvement if lower-noise circuitry could be devised. However, in neither case was the problem of magnetic interference considered. This problem, discussed in Section D, might well limit the useful sensitivity of a "nuclear gyro" well above the limit predicted by the statistical uncertainty relations quoted from reference 3.

C. C W NUCLEAR GYROSCOPES

1. General Description

In a continuous wave (CW) nuclear resonance experiment, the gross nuclear magnetization has a frequency response characteristic near resonance similar to that of an ordinary electrical

tank circuit. If the nuclear resonant frequency is determined in a stationary coordinate system, it is given by $\omega_o = \gamma H_o$ radians per second, where γ is the gyromagnetic ratio of the nuclear particles and H_o is the DC bias field. The effect of mechanically rotating an NMR experiment about the bias field axis at angular frequency $\Delta\omega$ can be represented by replacing H_o with $(H_o - \frac{\Delta\omega}{\gamma})$.[5] Consequently the apparent nuclear resonant frequency in a rotating system is shifted from the resonant frequency in a stationary frame by exactly the frequency of rotation.

A CW nuclear "gyro" could therefore be built from an oscillator and a discriminator, with the frequency of either the source or the discriminator controlled by a nuclear spin system. (Some additional advantage might be gained by using a nuclear spin system in both oscillator and discriminator, with their bias fields oppositely oriented, at the expense of increased bias field stability problems). The nuclear spin system used in the oscillator and/or the discriminator might represent either a passive component (i.e. like an electrical tuned circuit) or an active one. The following section discusses the use of NMR spin systems as passive elements in a CW nuclear gyro, and estimates a sensitivity limit for a typical case; Section C.3 describes possible applications of active nuclear resonance devices, or so-called "RASERs" to angular motion sensing. Problems of magnetic bias field stability and extraneous magnetic interference are discussed in Section D.

2. Passive Devices

A sample of material containing suitable nuclear particles, together with driving and sensing coils and a biasing magnet, would constitute a simple nuclear resonance "tank circuit" for use in either the oscillator or the discriminator of a CW nuclear gyro. If the driving and sensing coil axes are orthogonal so that the only coupling between them is through the nuclear magnetization, then the addition of an amplifier and a phase adjusting network connected between the

coils would allow the system to oscillate at the nuclear resonance frequency. If the instrument is mechanically rotated, then the frequency of the oscillator will change by the mechanical rotation frequency. This frequency shift, detected by a discriminator, would be the indication of mechanical angular rate. The same nuclear sample and coil arrangement could be used for a nuclear resonance discriminator, driven at its normal (i.e., non-rotating) resonant frequency by a constant-frequency oscillator and detecting mechanical rotation by means of the apparent shift in its resonant frequency when compared with the constant-frequency oscillator. To indicate sensitivity limits of such devices an approximate analysis for the "NMR discriminator" will be made below.

The response of the nuclear magnetization to a steady bias field H_z in the +z direction and an RF magnetic field in the (x, y) plane is described by the Bloch equations:[4]

$$\begin{aligned} \dot{M}_x &= \gamma (M_y H_z - M_z H_y) - \frac{M_x}{T_2} \\ \dot{M}_y &= \gamma (M_z H_x - M_x H_z) - \frac{M_y}{T_2} \\ M_z &= \gamma (M_x H_y - M_y H_x) - \frac{(M_z - M_o)}{T_1} \end{aligned} \qquad (2.25)$$

where (M_x, M_y, M_z) and (H_x, H_y, H_z) are the instantaneous components of the nuclear magnetization and the magnetic field, M_o is the equilibrium magnetization in the z direction, and the parameters γ, T_1, T_2 are the nuclear gyromagnetic ratio and the longitudinal and transverse relaxation times, respectively.

It is convenient, in the case of a circularly polarized RF driving field, to change to a coordinate system which rotates with the driving field vector. If the driving field is linearly polarized, then it can be regarded as the superposition of two counterrotating circularly polarized fields. If γ is positive (as in the case of protons) and the bias field is in the +z direction, then the nuclear magnetization

will tend to follow the circularly polarized component which rotates in the (-z) sense, and will see the other rotating component going by at twice its resonant frequency in the opposite direction. Since the nuclear susceptibility at twice resonant frequency is generally much smaller than at resonance, a useful approximate steady-state analysis of the nuclear magnetization in a linearly polarized driving field can be made by neglecting the counterrotating component and treating the driving field as though it were circularly polarized (of half its linearly polarized magnitude) and rotating in the proper sense to drive the nuclear particles at resonance. The Eq. 2.25 can be transformed into a coordinate frame rotating at angular velocity ω in the (-z) sense by replacing H_z, wherever it appears, with $(H_z - \frac{\omega}{\gamma})$.[5] Designating the rotating axes as x' and y', and choosing the x' axis to coincide with the rotating RF field of magnitude H_{RF}, the rotating magnetization components M_x' and M_y' can be found for the case of constant or slowly changing ω by setting the time derivatives $\dot{M}_x$, $\dot{M}_y$, and $\dot{M}_z$ equal to zero in the transformed equations. This leads to the solution

$$M_x' = (H_{RF}\ \gamma M_o T_2)\ \frac{T_2\ (\Delta\omega)}{1+\gamma^2 H_{RF}^2 T_1 T_2 + T_2^2 (\Delta\omega)^2}$$

$$M_y' = (H_{RF}\ \gamma M_o T_2)\ \frac{1}{1+\gamma^2 H_{RF}^2 T_1 T_2 + T_2^2 (\Delta\omega)^2}$$

$$M_z = M_o\ \frac{1+T_2^2 (\Delta\omega)^2}{1+\gamma^2 H_{RF}^2 T_1 T_2 + T_2^2 (\Delta\omega)^2} \qquad (2.26)$$

In the above equations, $\Delta\omega$ is the deviation from the nuclear resonance frequency ($\Delta\omega = \gamma H_z - \omega$) caused by mechanical rotation of the instrument, i.e., $\Delta\omega$ is the mechanical rotational speed around the z-axis.

The only component of magnetization in which there is a first-order change with $\Delta\omega$ is the component in phase with the driving field, M_x'. Consequently, to detect small angular rates $\Delta\omega$ it would be desirable to measure either the change in M_x' or the change in the phase angle between H_{RF} and the rotating component of magnetization, which is obtained from Eq. 2.26 as $\frac{\pi}{2} + T_2(\Delta\omega)$ radians, for small values of $\Delta\omega$. In either case the signal power available to the detector is supplied by the RF driving field, and coupled to the detector through the M_x' component of magnetization. An upper limit to the signal power available to the detector can be estimated by first, imagining the sensing coil to be open circuited and calculating the power supplied by the driving field. Then the sensing coil is connected to a detector, and power is extracted from the nuclear spin system. The resulting increase in RF driving power indicates an upper limit to the signal power available at the detector. The torque exerted by the RF field on the rotating magnetization is

$$\text{Torque} = H_{RF} M_y' = \frac{H_{RF}^2 \gamma M_o T_2}{1+\gamma^2 H_{RF}^2 T_1 T_2 + (T_2 \Delta\omega)^2} \qquad (2.27)$$

The RF power supplied to the nuclear magnetization is therefore

$$P_{RF}(\Delta\omega) = \omega(\text{torque}) \approx \omega_o(\text{torque}) = \frac{\omega_o H_{RF}^2 \gamma M_o T_2}{1+\gamma^2 H_{RF}^2 T_1 T_2 + (T_2 \Delta\omega)^2} \qquad (2.28)$$

If $(T_2\Delta\omega)^2 << 1 + \gamma^2 H_{RF}^2 T_1 T_2$, expression 2.28 simplifies to

$$P_{RF} = \frac{\omega_o H_{RF}^2 \gamma M_o T_2}{1+\gamma^2 H_{RF}^2 T_1 T_2} \left\{ 1 - \frac{(T_2 \Delta\omega)^2}{1+\gamma^2 H_{RF}^2 T_1 T_2} \right\} \qquad (2.29)$$

Equation 2.29 gives the RF power supplied to the nuclear magnetization vector, as a function of $\Delta\omega$, before any power is coupled out into a detector. When the detector is connected to the sensing coil and begins to extract power from the M_x' component of magnetization, then this magnetization component will decrease and the phase angle between H_{RF} and the rotating magnetization component will approach 90^o; that is, the angle $T_2\Delta\omega$ will decrease. Since $\Delta\omega$ does not change when the detector is connected to the sensing coil, the effective transverse relaxation time must decrease as a result of coupling energy out of the spin system. A new equilibrium would be reached with the magnetization lagging the RF field by the angle $\frac{\pi}{2} + T_2^*\Delta\omega$, where T_2^* is the effective transverse relaxation time when the radiation damping of the detector is included. Since the new equilibrium phase angle between the magnetization and H_{RF} is closer to $\frac{\pi}{2}$, the power supplied to the nuclear spins by the RF field is increased, due to the power extracted by the detector. The signal power available to the detector P_s, is at most equal to half this change in RF input power, or

$$\Delta P_s \leq \frac{1}{2}\left[P_{RF}(T_2^*\ \Delta\omega) - P_{RF}(T_2\,\Delta\omega)\right] \tag{2.30}$$

A less restrictive, but still useful upper bound on the available signal power can be obtained more easily by substituting for $P_{RF}(T_2^*\,\Delta\omega)$ the RF power supplied to the spin system at resonance and with no detector load, using for T_2 the natural (undamped)value. This is equivalent to assuming that all of the power contained in the M_x' component of nuclear magnetization could be removed from the nuclear spin system without decreasing the transverse relaxation time. Although these are physically inconsistent assumptions, they lead to a simple evaluation of an upper limit to the sensitivity of a CW nuclear gyro using a nuclear spin system as a passive discriminator. Employing the assumption discussed above, the signal power is

$$P_s \leq \frac{1}{2} \left\{ P_{RF}\,(\text{res.}) - P_{RF}\,(T_2\,\Delta\omega) \right\} \qquad (2.31)$$

For small angles $(T_2\,\Delta\omega)$, this is

$$P_s \leq \frac{\omega_o\, H_{RF}^2\, \gamma\, M_o\, T_2 (T_2\,\Delta\omega)^2}{2\,(1+\gamma^2\, H_{RF}^2\, T_1\, T_2)^2} \qquad (2.32)$$

Expression 2.32 reaches a maximum with H_{RF} when

$$H_{RF} = \gamma\,(T_1\ T_2)^{\frac{1}{2}}$$

This maximum value is

$$P_s \leq \frac{X_o\, V\, H_o^2 (T_2\,\Delta\omega)^2}{8\, T_1} \qquad (2.33)$$

In the above expression the substitutions $M_o = X_o\, V\, H_o$, and $\omega_o = \gamma H_o$ have been made, where X_o is the static nuclear magnetic susceptibility per unit volume, and V is the sample volume. To remain consistent with the detection criterion of Section B, the "detection threshold" will be assumed to occur at a (power) signal to noise ratio of four. With an equivalent input noise level of N_o watts per cps and a bandwidth B cps, the minimum detectable angular rate would then be

$$(\Delta\omega)_{min} \geq \frac{4}{T_2\, H_o} \left(\frac{2\, T_1 B N_o}{X_o\, V} \right)^{\frac{1}{2}} \qquad (2.34)$$

To evaluate this limit for a typical example, the case of proton resonance in water at room temperature will be considered. The transverse relaxation time, T_2, may be restricted to comparatively low values due to dynamic performance requirements of the instrument; in this sample numerical calculation this will be disregarded. The static nuclear susceptibility for protons in water is about 3×10^{-17}

joules per (gauss)^2 per (cm)^3, and $T_1 \approx T_2 \approx 3$ seconds. Assuming a sample volume of 10 cm^3, a bandwidth of ten cps, an input noise level of 3×10^{-18} watts per cps as used in Section B and a bias field of 3500 gauss (for a resonance frequency of about 15 megacycles), Eq. 2.34 gives an upper limit to the minimum detectable angular rate as

$$(\Delta \omega)_{min} \geq 3 \times 10^{-4} \text{ radians per second.} \qquad (2.35)$$

This is a rather optimistic estimate for the sensitivity, due both to the approximation of Eq. 2.31 and the assumption that T_2 could be kept at the natural value regardless of system dynamic requirements. The exact maximum allowable value for T_2 would depend on the particular dynamic response desired from the system to which the instrument is connected, as well as the characteristics of other system components, but would most likely be shorter than the value of three seconds used here. It is apparent that a change in the excitation frequency would appear to the instrument as an angular rate input, as would a change in H_o. For these reasons, the stability of the excitation frequency and the bias field (and the exclusion of external magnetic interference) would present difficult problems and might limit the useful sensitivity of the device to a value considerably less than that predicted solely on the basis of signal strength and amplifier noise level.

The NMR oscillator suggested earlier would be subject to similar limitations. An additional factor in its analysis would be the fact that, while the power that can be transferred through the nuclear spin system generally increases with increasing bias field, and therefore the oscillator power output would increase as well, the resonant frequency also increases and makes the construction of a discriminator with sufficiently narrow bandwidth to detect small changes in the oscillator frequency more difficult.

3. Active Devices

The sample calculation of the preceding section for a nuclear spin system used as a passive circuit element in a discriminator illustrates the fact that the amount of RF power that can be coupled through the nuclear magnetization of a reasonable volume of material at ordinary temperatures is small. Whether the nuclear spin system is used in an oscillator or a discriminator, the same problem, in varying degrees, arises. That is, there is at least one point in the "gyro" circuitry where the RF signal must be transmitted through the nuclear spin system, suffering a high attenuation and producing a low level output. It is felt that the problem of accurate detection and processing of these signals in the presence of typical electronic noise levels represents a serious obstacle to the construction of a nuclear gyro capable of a sensitivity comparable to that of conventional gyroscopes.

The problem of detecting small nuclear signals discussed above can be alleviated to a considerable extent by operating the device in a way in which an RF power gain is achieved through the nuclear spin system. This requires a means of "pumping" energy into the nuclear spins so that the population of the higher energy level exceeds that of the lower, as in a MASER. Such a means of pumping is provided by the Overhauser effect in a liquid containing paramagnetic impurities[9] which is a coupling between electronic and nuclear magnetic transitions that allows the population of the higher nuclear energy state to exceed that of the lower when power is supplied at the frequency of the electron magnetic transition. This effect was demonstrated experimentally in 1957[10] and was recently employed in the construction of a "MASER" oscillator at the National Company, Inc.[11] The device converts microwave power at the electron magnetic transition frequency into RF power at the nuclear resonance frequency, and hence is termed a "RASER."

This ability to obtain an RF power gain or, when coupled to a resonant tank circuit of sufficiently low loss, an oscillator, through the nuclear spin system appears to offer the possibility of circumventing the signal to noise ratio problem present in detecting the small signals transmitted through a "passive" nuclear spin system. If so, the potential sensitivity of a nuclear gyro utilizing a "RASER" might ultimately be limited by the random fluctuations or "noise" of the energy conversion processes occurring within the nuclear sample rather than by the noise level of the associated electronics. This inherent "nuclear noise" produces a frequency uncertainty in a RASER oscillator, which was calculated by Mssrs. Ganssen and Sloan of the National Company to be about 8 parts in 10^{11} at 15 mcs, for a natural resonance line width of 100 cps. For a line width of 10 cps which can be achieved with moderate effort, the uncertainty in oscillator frequency would be about 8 parts in 10^{13}, or around 10^{-4} radians per second. These frequency deviations were calculated according to the theory of microwave MASERS,[12] using values of the parameters measured experimentally on the devices constructed at the National Company.

The bandwidth figures quoted above indicate that with additional development effort the frequency uncertainty of a "RASER" oscillator might be reduced to the order of an earth rate (exclusive of magnetic bias field variations). Since such a device also can be made to provide enough power to avoid the interference from detector noise levels which would limit the usefulness of "passive" NMR devices, it appears that a combination of a "RASER" oscillator and a "RASER" amplifier (operating in separate, oppositely directed bias fields) might have the potential of achieving a sensitivity to mechanical rotation of the order of an earth rate. This would require very stable bias fields, as discussed in Section D.

D. MAGNETIC SHIELDING

In Chapter I it was pointed out that the effects of mechanical rotation on the motion of magnetic particles can be represented by an equivalent magnetic field, proportional to the speed of mechanical rotation. The devices discussed in this chapter, which attempt to detect mechanical rotation by measuring these small equivalent magnetic fields, must be protected from external magnetic fields to prevent false indications of mechanical rotation. Adequate magnetic shielding is consequently an important practical problem in the construction of an angular motion sensor operating on this principle. Suitable shields might be made from a high permeability material or from a superconducting metal. Some advantages might also be gained from a combination of the two types.

High permeability shields are commonly used in electronic gear or instruments sensitive to magnetic interference, to provide a low reluctance path for the magnetic flux to bypass the region to be shielded. Mumetal shields can reduce the magnetic field in their interior to perhaps around 10^{-4} or 10^{-5} gauss. This residual field appears to be associated at least in part with the mumetal itself, so it is doubtful if the degree of shielding could be improved substantially by increasing the thickness of the shield or decreasing the cavity size.

Closed surfaces made of superconducting materials of ordinary purity maintain the magnetic flux penetrating the surface at a constant value, by virtue of the absence of electrical resistance, which allows surface currents to be generated and indefinitely maintained to compensate for any changes in external magnetic flux. This situation obtains as long as the external field does not exceed a certain level, at which the material changes to the normal (non-superconducting)state. The critical field at which this transition takes place is a function of the material and of its temperature, and is tabulated in Reference 13 for several materials.

Meissner discovered[14] that the magnetic flux penetrating a superconductor of sufficient chemical and structural purity was very small, and theorized that the flux would be exactly zero within a superconductor entirely free from chemical impurities and structural defects. It is now thought that the magnetic flux initially linking a superconductor when in the normal state is forced out of the superconducting material when the transition to the superconducting state takes place, but that flux may congregate in a region of impurities until the critical field is exceeded within that region and a small part of the material remains in the normal state when refrigerated. When the remaining material around the impurities changes into the superconducting state, the flux passing through the impurity regions is trapped, and it is this trapped flux associated with impurities which produces the residual field measured within superconducting shields. The size of this residual field is an indication of the purity of the material and its structural uniformity, and a residual field of around 10^{-6} gauss is about the best currently obtainable.[15] A theoretical interpretation of these properties of superconductors can be found in, for example, reference 17.

Recent experiments[16] indicate that the total flux enclosed within a superconductive loop is quantized in units of about 2×10^{-7} maxwells. Consequently, it appears that if a superconducting material is refrigerated in a region in which the total flux is less than 2×10^{-7} maxwells, a truly "perfect" shield, with no entrapped flux, might be obtained.

It was pointed out that chemical purity is essential to achieving a small residual flux. Superconducting materials composed of a single pure element, however, normally have a low critical field in contrast to those superconducting alloys which are frequently used in the construction of superconducting magnets, where a high critical field is required and where residual field is not especially important. Consequently, where a pure element superconductor is required for low residual field applications it may be necessary to surround the

superconducting shield with a high-mu shield to prevent its critical field from being exceeded due to external magnetic fluctuations. This combination of a superconductor surrounded by a high-mu shield should provide a residual field of around 10^{-6} gauss with current technology and with the possibilities for improvement indicated by the flux quantization effect.

One scheme which has been proposed to reduce the effect of magnetic interference on a nuclear gyro involves the use of two nuclear species, with different gyromagnetic ratios, mixed together in the same sample. The nuclear precession signals from both types of nuclei are detected. Since any interfering magnetic field would act differently on the two nuclei, while the frequency shifts due to mechanical rotation would be the same for both types of nuclei, the two signals can be combined to compute the mechanical rate independent of magnetic interference. This arrangement requires detecting the two signals separately and then combining the two output indications with the proper scale factors, determined by the two gyromagnetic ratios. In this way the errors resulting from magnetic interference can be reduced by a factor of roughly the relative accuracy of the scale factors used in combining the two signals. This improvement is obtained at the expense of additional electronic complexity.

E. CONCLUSION

Because of the small magnetic moments of nuclei, and the resulting small susceptibilities, the energy which can be stored in a nuclear spin system and subsequently coupled to a detector by mechanical rotation is very small. One of the major problems of workers in the NMR field has been the construction of sufficiently sensitive electronic apparatus to detect and display the nuclear resonance signals, and several variations from the conventional amplifier have been used. Some of these schemes are described in References 6 and 7. These very small power levels make the

prospects of constructing a "nuclear gyro" utilizing a nuclear spin system as a passive element discouraging.

The possibilities of a nuclear gyro using a nuclear spin system as an active element, as discussed briefly in Section C. 3 are more encouraging. Here, additional coupling mechanisms operate to produce an equivalent susceptibility much higher than the static value.

Any variety of "nuclear gyro" whether passive or active, would be subject to the same restrictions regarding interference from extraneous magnetic fields. Any extraneous magnetic field, or a change in a DC bias field, of magnitude ΔH, would produce an indication of an apparent output rate equal to $\gamma \Delta H$. Since the gyro-magnetic ratio, γ, of most nuclear particles is in the range of a few kilocycles per gauss, it is apparent that an instrument capable of detecting an earth rate, for example, would have to be shielded against stray fields down to around 10^{-8} gauss. This also applies to time variations in the DC biasing field used in a CW nuclear gyro.

The limitation on sensitivity imposed by shielding requirements is felt to be perhaps an earth rate, as an optimistic estimate; the signal to noise ratio limitation for a passive nuclear gyro is probably in the same order of magnitude. It is not clear what effects would ultimately limit the sensitivity of an active nuclear gyro (a "NMR MASER"), other than the common problem of magnetic interference. If a perfect superconducting shield could be devised then an active nuclear gyro might approach the sensitivity of current conventional gyros. However, such a device would require extensive peripheral equipment including a refrigerator for the shield, a microwave power source for the "pump," highly stable biasing magnets and an elaborate signal detection and processing system. It is felt that the relatively poor sensitivity, in comparison with that obtainable with conventional gyroscopes, does not warrant extensive development work on a nuclear gyroscope.

CHAPTER III

MICROSCOPIC CORIOLIS FORCE SENSORS

A. INTRODUCTION

The Faraday Effect and Nuclear Magnetic Resonance studies indicate that the output of possible microscopic particle gyroscopes increases with the mass to charge ratio of the particles used. This chapter is concerned with an investigation of microscopic particles with mass to charge ratios greater than that characteristic of atomic systems. In particular, molecular and colloidal particles are investigated within the framework of possible devices utilizing them as gyroscopic media.

We wish to drive a molecular or colloidal system with an angular rate Ω_o and detect a signal, (electric, magnetic or other,) indicative of the drive rate. A mechanical rotation can affect the system in essentially two ways, through centrifugal and Coriolis forces.

$$F_{cent} = m\,\vec{\omega} \times [\vec{\omega} \times \vec{r}]$$

$$F_{cor} = 2m\,\vec{v}' \times \vec{\omega}$$

If we wish to detect a rate Ω_o, the force must take the form;

$$F = m[2\vec{v}' - (\vec{\Omega}_o \times \vec{r})] \times \Omega_o$$

where $\vec{v}'$ and $\vec{r}$ are present independent of Ω_o. Since $\vec{\Omega} \times \vec{r}$ represents a velocity we can include it with $\vec{v}'$, so that we have

$$F = 2m\,\vec{v} \times \Omega_o; \qquad (3\text{-}1)$$

where m is the particle mass, Ω_o is the input we wish to detect and $\vec{v}$ is an input velocity. In the following devices we will excite the system of particles

to give them a velocity in the y-direction. The angular rate we wish to detect will be assumed to be in the z-direction. The output we detect will then be the x-direction, in accordance with Eq. 3-1. We will assume that the output motion does not, in turn, affect the input y-directed velocity because it is so much smaller than the excitation velocity.

B. MOLECULAR SYSTEMS

1. Bound Particles

The first case we will consider is a system of bound molecular particles, such as exists in the lattice of a solid. The excitation will be an oscillating electric field. We shall assume that all particle motions are small such that we can consider the lattice forces as being linear. The model used is shown in Fig. 3.1.

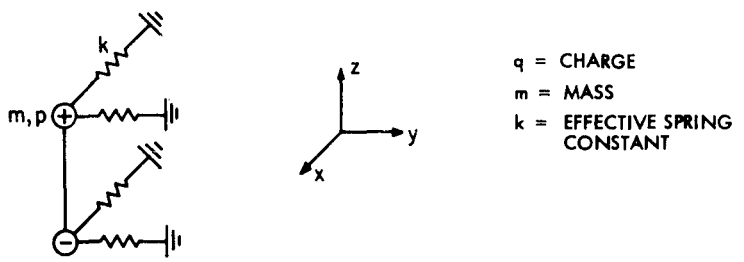

Fig. 3.1 Simple Model for a Polar Solid

For the input velocity v_y, we have the following for a balance

$$F_{elec.,\,y} = F_{restoring,\,y}$$

$$qE_y = ky$$

Here y is the displacement in the y-direction. If $E_y = E_o \cos \omega_o t$, $v_y = \dot{y}$ becomes

$$|v_y| = \frac{\omega_o |E| q}{k}$$

where || indicates the magnitude of a sinusoidal quantity. If $\vec{r}$ is $\Omega_o \vec{i}_z$, the output Coriolis force from Eq. 3-1 becomes;

$$|\vec{F}_{cor}| = \frac{2 m \omega_o |E| q}{k} \vec{i}_x$$

$$F_{restoring, x} = F_{cor, x}$$

so that the displacement in the x-direction |x| is,

$$|x| = \frac{2 m \Omega_o \omega_o |E| q}{k^2} \tag{3-2}$$

We detect this displacement by measuring the electric polarization resulting from the relative motion of plus and minus charges. This polarization is given by

$$|P_x| = \frac{q \times N_o}{\epsilon_o} \frac{\text{volts}}{\text{meter}} \tag{3-3}$$

Combining Eq. 3-2 and 3-3 we get,

$$|P_x| = \frac{2 m \Omega_o \omega_o |E| q^2 N_o}{\epsilon_o k^2} \tag{3-4}$$

N_o = number of dipoles per unit volume and ϵ_o is the free space susceptibility. We have assumed throughout that the drive frequency ω_o is very much smaller than the particle natural frequency.

It is desirable to express Eq. 3-4 in terms of directly physically measurable quantities. Towards this end we will proceed to derive an

expression for χ, the relative electric susceptibility, using the same simple model of Fig. 3.1. Equation 3-4 will be expressed in terms of χ. This will also hopefully, account for some of the gross simplifications embodied in the model of Fig. 3.1, in that the value used for χ will be a measured quantity that presumably will reflect the factors not considered in the model.

$$\chi = \frac{P_{resultant}}{E_{applied}}$$

where $E_{applied}$ and $P_{resultant}$ are in the same direction. The displacement x,

$$x = \frac{q\,E_{applied}}{k}$$

and the polarization from Eq. 3-3

$$P_{resultant} = \frac{N_o q^2}{\epsilon_o k}\; E_{applied}$$

Therefore

$$\chi = \frac{N_o q^2}{\epsilon_o k} \tag{3-5}$$

If we also define a natural frequency

$$\omega_n \triangleq \sqrt{\frac{k}{m}} \tag{3-6}$$

for the system Eq. 3-4 becomes

$$|P_x| = \frac{2\,\Omega_o\,\omega_o}{\omega_n^2}\,\chi|E| \qquad \frac{\text{volts}}{\text{meter}} \tag{3-7}$$

which we shall use as for evaluation as a possible angular rate detector.

$|E|$ = Input electric field (10^5)

Ω_o = Angular rate (10^{-4})

ω_o = Freq. of input field (10^6)

$|P_x|$ = Output polarization

χ = relative susceptibility of material (100)

ω_n = natural resonant (10^{12}) frequency of molecules

Shown in parenthesis are typical M.K.S. values for the parameters. For these values P_x is of the order of 2×10^{-15} $\frac{\text{volts}}{\text{meter}}$ for one earth's rate input. The small size of this signal is attributed to the strong lattice restoring forces. The elastic constant k is electrostatic in nature and therefore is proportional to q^2. From Eq. 3-6 ω_n is proportional to q and inversely proportional to the square root of the mass. From Eq. 3-5 χ is independent of q. Therefore P_x is proportional to $\frac{m}{q^2}$. The above relationship is similar to the $\frac{m}{q}$ dependence found in the atomic systems previously considered. In the following cases this sort of dependence will be replaced by an mq product relation. The difference arises in the assumptions made in the models used. In the atomic systems and the molecular system just considered electric or magnetic restoring forces were treated as the chief limitation. This is not the case for the following systems.

Next we shall try to free the molecule from the strong lattice forces by considering a fluid or gas. In this state the electric restoring force limitation is eliminated, allowing larger outputs. However, thermal considerations will provide an upper limit on the output we can achieve.

2. Free Particles

The small output achieved in the device just considered can be attributed to large binding (lattice) restoring forces (Eq. 3-4). We shall now consider another large class of particles, those which are nondirectly interacting but whose motions are governed chiefly by thermal considerations. Such a situation exists in most polar liquids and gases. Again we will assume a simple model

(Fig.3.2), drive with a y-directed oscillating electric field and detect a motion in the x-direction. Hopefully these particles will provide larger outputs since they have been freed from the strong lattice forces.

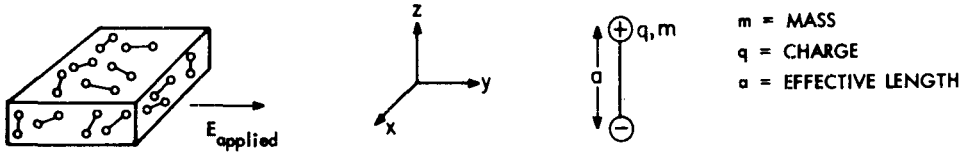

Fig. 3.2 Simple Model for a Polar Fluid

The analysis is simplified by assuming only six possible dipole states, aligned in the $\pm x$, $\pm y$, or $\pm z$ directions. This assumption will not introduce an order of magnitude error. We can use a Maxwell-Boltzman state distribution. $p_{\pm x}$ the probability of finding a dipole oriented in the $\pm x$ direction is given by;

$$p_{\pm x} = A\, e^{\frac{W_{\pm x}}{kT}}$$

where $W_{\pm x}$ is the energy associated with $\pm x$ direction, A is a normalizing coefficient, T is the absolute temperature and k is Boltzman's constant. Similar expressions exist for $p_{\pm y}$ and $p_{\pm z}$. In our case,

$$W_{\pm y} = q\, a\, E \cos \omega_o t$$

$$W_{\pm z} = 0$$

$W_{\pm x}$ = Work done by Coriolis force while aligning a particle in the x-direction = $F_{coriolis}\, a$

$E \cos \omega_o t$ = applied field

The mean charge displacement in the y-direction caused by the applied field is

$$y = a(p_{+y} - p_{-y})$$

If we make the assumption that $W_{\pm x} \ll kT$ then A becomes $\approx \frac{1}{6}$ and y becomes

$$y = \frac{a^2 q E \cos \omega_o t}{3\,kT} \quad , \qquad \dot{y} = v_y = \text{velocity in y-direction}$$

$$|v_y| = \frac{\omega_o a^2 q|E|}{3\,kT}$$

where again || indicates sinusoidal magnitude. This should be interpreted as a mean particle velocity and not necessarily as an actual particle velocity.

$$|W_{\pm x}| = |F_{coreolis}|\, a = 2\, m\, r_o |v_y| a$$

$$= \frac{2\, m \Omega_o a^3 q|E|}{3\,kT}$$

Again we can interpret this as an average rather than necessarily having any particular physical significance. The net polarization in the x-direction is given by,

$$|P_x| = N_o^{1/3}\, q\, a\, [p_{+x} - p_{-x}] \tag{3-8}$$

N_o = number of particles per unit volume. Substituting the appropriate relations for p_{+x} and p_{-x} and assuming $W_{\pm x} \ll kT$ we obtain;

$$|P_x| = \frac{4q^2 a^4 m \omega_o \Omega_o (N_o)^{1/3} |E|}{3(kT)^2 \epsilon_o} \tag{3-9}$$

Again it is desirable to express $|P_x|$ in terms of the susceptibility χ.

$$\chi = \frac{P_{resultant}}{E_{applied}} \quad ; \quad W_{\pm} = \pm \frac{aq\, E_{app}}{kT}$$

Using Eq. 3-8 and assuming $W_{\pm} << kT$ we get;

$$\chi = \frac{(aq)^2 N_o}{\epsilon_o kT} \tag{3-10}$$

Combining Eq. 3-9 and 3-10

$$|P_x| = \frac{4a^2 m \omega_o \Omega_o}{3\, kT} \chi |E_o| \quad \frac{volts}{meter} \tag{3-11}$$

a = effective molecule size (10^{-8})

m = mass ($2x10^{-25}$)

ω_o = drive frequency (10^6)

χ = relative susceptibility (100) of material

E_o = input field (10^5)

Ω_o = angular rate (10^{-4})

k = Boltzmann's const

T = absolute temp (100)

$kT \approx 10^{-21}$

Typical M.K.S. values of the parameters are shown and give

$$|P_x| \approx 8x10^{-11} \quad \frac{volts}{meter}$$

Since χ rises as $\frac{1}{T}$, output increases inversely as temperature squared. However, if the temperature gets too low the assumed Maxwell-Boltzmann

distribution must be replaced by a different distribution which will cause the output to reach an upper limit as $T \to 0^{\circ}K$ and then decrease as the temperature is lowered still further, so that we cannot achieve a detectable output by sufficiently lowering the temperature.

3. Conclusions

It is important to note that the mass to charge ratio no longer imposes the chief limitation in a liquid or gas system. In fact $|P_x|$, the output, is proportional to $m\,q^2$ (Eq. 3-9). The chief limitation is now imposed by thermal considerations. In the solid, lattice binding energies, which are dependent on q, are large compared with thermal energies, therefore an $\frac{m}{q}$ functional relation appeared. When we tried to remove lattice forces, an improvement was obtained, however thermal effects imposed an upper limit, still well below detectable signals, for one earth's rate.

Colloidal size particles will be considered next. These have a much larger mass to charge ratio than molecules; however, again electric forces will not be the limiting factor, so that we will not obtain outputs increased by the increase in mass-to-charge ratio.

C. COLLOIDS

Any particles larger than a molecule but still microscopic can be considered as being colloidal. Of particular interest is a colloidal suspension which is a large number of like charged colloidal size particles in a suspending agent. Their charge prevents them from coagulating to form larger particles, and thus they can exist in a stable state. Unlike molecular solutions, colloidal particles in suspension have their charge adhering to their surface, rather than being chemically bonded. Therefore, a given suspension will contain particles of various size and charge. This nonuniqueness property prevents exact classification; however, most authors consider any stable state of particle from size 10^{-8} meters to 2×10^{-5} meters as being colloidal.

Since it has become apparent that mass to charge ratio is important in small particle gyroscopic phenomena, colloidal particles should be considered. A typical gold suspension particle of size 2×10^{-7} meters has a mass to charge ratio of 4×10^{-2} in M.K.S. units; compared with 6×10^{-12} for an electron and

1.2×10^{-8} for a proton. The electron and proton systems previously considered showed a sensitivity proportional to $\frac{m}{q}$ so colloidal particles offer the possibility of a million-fold improvement. However, as in the molecular systems considered before, this increase cannot be realized.

A suspended particle can be represented as shown in Fig. 3.3. Electric charges adhere to the surface of the particle and charges of the opposite

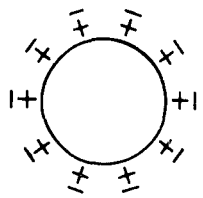

Fig. 3.3 Colloidal Particle

sign position themselves to form a double layer of charges such that an electric field can cause a relative motion between the particle and suspending media. Most authors prefer to speak of the electrokinetic potential drop across the double layer of charges, (Fig. 3.4), rather than the total charge on the particle. This is because ξ is essentially independent of particle size and dependent on only the nature of the substances involved.

Colloidal particles interact with electric fields through the so called Electrokinetic effects,* of which there are four, all governed by the same

---

* Electrokinetic Effects

1. Electrophoresis--Movement of solid particles with respect to the liquid; produced by an applied E.M.F.
2. Electroosmosis--Movement of liquid with respect to particles fixed in a porous diaphragm; produced by an applied E.M.F.
3. Sedimentation Potential--(reverse of electrophoresis) E.M.F. produced by movement of particles with respect to liquid (Dorn Effect)
4. Steaming Potential--(reverse of electroosmosis) E.M.F. produced by movement of liquid with respect to particles fixed in a porous diaphram.

relation. The form suited for our use is given by Eq. 3-12.[18,19]

$$V_{1,2} = \frac{\xi D P}{6\pi \eta k} \tag{3-12}$$

where η, D and k are the viscousity, dielectric constant, and specific conductivity of the fluid. ξ is the electrokinetic potential between a particle and the fluid, P is the hydrostatic pressure difference between the points 1 and 2 where the output voltage $V_{1,2}$ is being measured, and 6π is the coefficient for spherical particles. As an illustration of the use of Eq. 3-12 let us consider the electrokinetic phenomena known as the Sedimentation potential, or Dorn effect. If charged colloidal particles are allowed to fall through a resistive media under the influence of gravity, and electric field results in the direction of motion. The total potential between two points is given by Eq. 3-12. The gravitation force on the paricles produces a pressure gradient in the fluid by virtue of the fact that the fluid must support the weight of the falling particles. This pressure difference between two points 1 and 2 is given by;

$$P_{1,2} = m g N_o d \tag{3-13}$$

where g is the gravitational constant, d is the distance between points 1 and 2 and N_o is the number of particles per unit volume. In a colloidal particle gyro the gravitational force will be replaced by a Coriolis force. The particles are given a velocity, and an angular rate is applied orthogonal to the velocity. A Coriolis force will result, orthogonal to both the velocity and angular rate, (Eq. 3-1) producing the desired pressure gradient within the fluid. In the device shown in Fig. 34 the particles are assumed to have a large relative magnetic permeability. A magnetic field gradient is used to give the particles a y-directed velocity. Since the inertial-viscous time constant is small we can equate magnetic force to viscous drag.

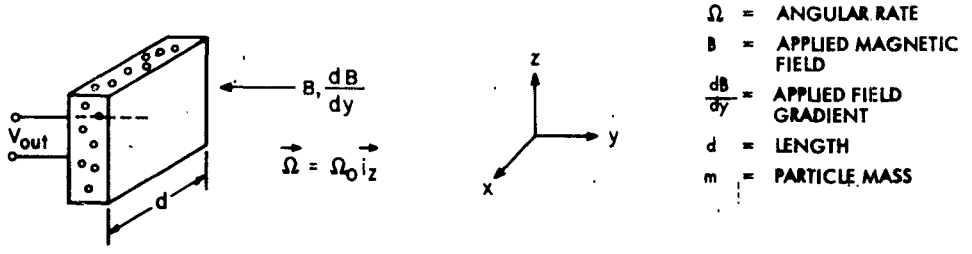

Fig. 3.4 Device Utilizing Colloidal Particles

$$F_{mag} = F_{viscous}$$

Using Stokes Law,

$$F_{viscous} = 6\pi a \eta v$$

and

$$F_{mag_y} = - \frac{\partial \text{Energy}}{dy}$$

where

$$\text{Energy} = \frac{1}{2} \frac{\mu B^2}{\mu_o^2} \quad \text{(volume)}$$

there results;

$$v_y = \frac{2\mu B \frac{dB}{dy} a^2}{q \mu_o^2 \eta} \tag{3-14}$$

a = particle radius

μ = particle magnetic permeability

μ_o = free space permeability

v_y = velocity in y-direction

The Coriolis force in the x-direction from Eq. 3-1 is given by,

$$F_{cor,x} = 2 m \Omega_o v_y \tag{3-15}$$

This force on each particle will result in a pressure difference between the x-end plates, similar to that in Eq. 3-13.

$$P = F_{cor,x} N_o d \tag{3-16}$$

where N_o = number of particles per unit volume. Combining Eq. 3-21 with 3-16 and using the fact that $m N_o = \rho a$ where ρ = particle density and a = particle concentration we obtain an expression for V_{out}

$$V_{out} = \frac{2\Omega_o}{27\pi} \quad \frac{Dd}{\eta^2 k} \quad \frac{B\frac{dB}{dy}}{\mu_o^2} \quad \rho a^2 a\mu \text{ volts} \tag{3-17}$$

Ω_o = angular rate (10^{-4})

D = fluid dielectric constant ($6x10^{-11}$)

η = fluid viscousity ($5x10^{-4}$)

k = fluid specific conductivity (10^{-4})

B = mag. field (.1)

$\frac{dB}{dy}$ = mag. field gradient (10)

μ_o = free space mag. ($1.2x10^{-6}$) permeability

ξ = electrokinetic potential (100 mv)

ρ = particle density (10^4)

a = particle radius (10^{-6})

a = particle concentration (.01)

μ = particle magnetic (1000 μ_o) permeability

d = device length (.1)

Typical or optimistic parameter values in M.K.S. units are shown. They give V_{out} $4x10^{-10}$ volts for one earth rate. It is very doubtful that much improvement could be achieved. The situation is complicated by the high output

impedance (1 Meg.), and the incompatibility of various parameters; for instance, it is difficult for a high electrokinetic potential colloid to exist in a concentrated form. Also, it is doubtful that the full V_{out} expressed in Eq. 3-12 can be realized. The Electrokinetic phenomena that we are utilizing is known as the Dorn effect.[21] Only very little work has been done on it and for the most part has been only qualitative.[20]

Equation 3-17 is proportional to ρa^2 and therefore increases with increasing mass. The output also increases with ξ which is equivalent to charge, so that the output increases with mass-charge product, not mass-to-charge ratio as was at first hoped. An increase in output proportional to mass-charge ratio can be expected only if electric restoring forces represent the chief limitation. This was the case in the atomic and bound molecule systems considered. However, this was not so in the free dipole configuration, and likewise is not so in the consideration of colloidal particles. In the derivation of Eq. 3-12 it was assumed that the output electric field produced by the displacement of charges did not affect the development of this field. This was because in all practical colloidal suspensions, the particle concentration is so low and the fluid viscousity is so high that the equivalent electrical output impedance of the particles is much higher than the electrical impedance offered by the suspending media. Therefore the derivation considers the moving particles as essentially a current source in a resistive media.

D. CONCLUSION

In electronic and proton systems, and some molecular systems (solids) the limiting factor for use as a gyroscope was electric or magnetic restoring forces, making the mass-to-charge ratio of the particle used important. In other molecular systems (liquids and gases) and colloidal systems, electric and magnetic forces can be neglected compared to other factors such as thermal or viscous effects. As we go to larger particles we cannot expect an improvement proportional to mass-to-charge ratio increase.

CHAPTER IV

FLUID GYRO

A. INTRODUCTION

The basic objective of this study of bulk fluids is to determine if any of their properties can be used in the establishment of a coordinate system which is fixed in inertial space and thus is independent of the orientation of its immediate environment. An apparatus is conceived in which a sphere filled with a liquid of low kinematic viscosity would exhibit only a very slight coupling between fluid and container. The degree to which the fluid would remain fixed in inertial space would be a function both of its kinematic viscosity and of the characteristics of the input motions applied to the container. If a fluid can be found in which the inertial fixation is satisfactory for practical input signals, and if the inertial coordinate system existing in the interior of the fluid can be made observable, then it is possible to realize a "gyroscope" with no rotating member which is sensitive to input angular motions about any axis.

As indicated above, two separate criteria must be met if a device such as that described is to be realized. The first of these is that the liquid must indeed be shown to remain fixed in inertial space to a satisfactory degree, and the second is that the inertial coordinates thus established must in some way be made observable. Clearly, the first of these represents the more fundamental limitation, for the desired effect must be shown to be present before the implementation of sensing means can begin. This is not to imply that such implementation to the required sensitivity may not represent a major problem; it is a problem here distinguished in kind, not necessarily in degree.

It is intuitively clear that to some extent the interior portions of a fluid will exhibit decoupling from the motions of the container. It is apparent also that the decoupling will be greater as the kinematic viscosity (ratio of viscosity to density) is decreased and as the apparatus size is increased such that the ratio of surface area to volume is diminished. The quantitative aspects of these effects are here investigated with the intent of describing their properties

in functional form and of ascertaining the degree to which the first criterion stated above can be met. The problem of detecting the motion of the fluid with respect to the container was not investigated.

B. ANALYSIS

The equations of motion of the fluid were derived and solved in rectangular and cylindrical coordinates for two types of input, an applied step and an applied sinusoid. The geometry and relevant dimensions are shown in Fig. 4.1 together with the differential equation of motion applicable in each coordinate system.

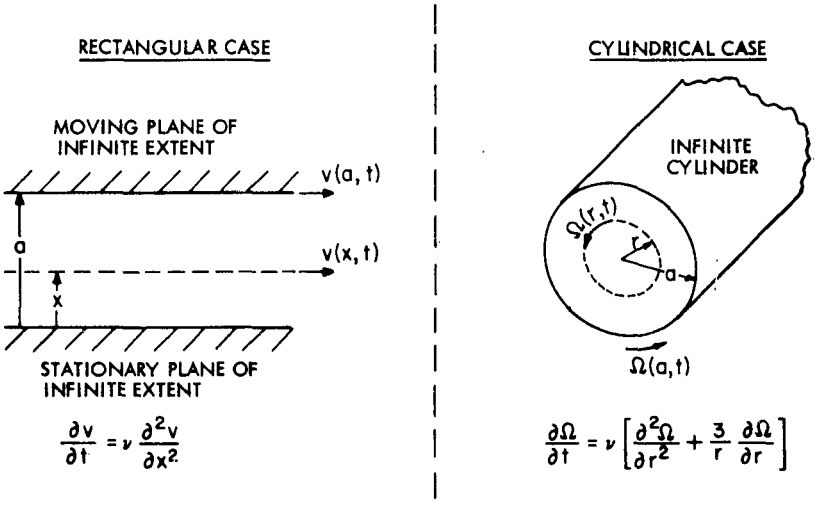

Fig. 4.1 Geometry and Equations of Motion

The differential equations above are the Navier-Stokes equations for the motion of a viscous fluid, and as such they are strictly applicable only to laminar flow. This restriction is not a severe one for present purposes, but the effects of turbulence must be considered if the input rates and accelerations

are such as to lead to fluid shears which will initiate turbulent flow. In particular, the use of any mechanical scheme for sensing must be investigated in terms of the turbulence it will introduce.

The equation in the rectangular geometry is simply the diffusion equation. The equation in the cylindrical geometry is reducible by a proper change of variable to Bessel's equation.[22] The equations of motion were not set up and solved in a spherical geometry due to a considerably increased mathematical complexity. It is felt that the results in the rectangular and cylindrical cases are generally representative of the spherical case also, making the omission of little consequence. The analytical solutions for the four cases which were considered appear below.

1. Rectangular Coordinates: Step Response
   [Fluid initially at rest; $v(a,t) = V_o\, U_{-1}(t)$]

$$\frac{v(x,t)}{V_o} = \left[\frac{x}{a} - \frac{2}{\pi} \sum_{n=1}^{\infty} \frac{(-1)^{n+1} \sin \frac{n\pi x}{a}}{n} e^{-\nu n^2 \pi^2 t/a^2}\right] u_{-1}(t) \tag{4.1}$$

2. Rectangular Coordinates: Steady State Frequency Response
   [$v(a,t) = V_o \sin \omega t$]

$$\frac{v(x,t)}{V_o} \quad V_M \sin(\omega t + \theta) \tag{4.2}$$

where

$$V_M = \left[\frac{\cosh^2 k_1 x - \cos^2 k_1 x}{\cosh^2 k_1 a - \cos^2 k_1 a}\right]^{1/2}$$

$$\theta = \operatorname{Arg}\left[\frac{\sinh k_1 x(1+j)}{\sinh k_1 a(1+j)}\right]$$

$$k_1 = \left(\omega/2\nu\right)^{1/2}$$

3. Cylindrical Coordinates: Step Response
[Fluid initially at rest; $\Omega(a,t) = \Omega_o u_{-1}(t)$]

$$\frac{\Omega(r,t)}{\Omega_o} = \left[1 + 2 \sum_{n=2}^{\infty} \frac{J_1(a_N r/a)\, e^{-\nu a_N^2 t/a^2}}{(a_N r/a)\, J_o(a_N)} \right] u_{-1}(t) \tag{4.3}$$

where a_N are the roots of $J_1(a_N) = 0$

4. Cylindrical Coordinates: Steady State Frequency Response
[$\Omega(a,t) = \Omega_o \sin \omega t$]

$$\frac{\Omega(r,t)}{\Omega_o} = \Omega_M \sin(\omega t + \theta) \tag{4.4}$$

where $$\Omega_M = \left(\frac{a}{r}\right) \left[\frac{\mathrm{ber}^2(K_2 r) + \mathrm{bei}^2(K_2 r)}{\mathrm{ber}^2(K_2 a) + \mathrm{bei}^2(K_2 a)} \right]^{1/2}$$

and $$\theta = \mathrm{Arg} \left[\frac{\mathrm{ber}(K_2 r) + j\,\mathrm{bei}(K_2 r)}{\mathrm{ber}(K_2 a) + j\,\mathrm{bei}(K_2 a)} \right]$$

$$K_2 = (\omega/\nu)^{1/2}$$

Despite the rather formidable appearance of these expressions, particularly in the cylindrical case, a plot of the solutions appears remarkably as one would expect. Significantly, it is found that with the use of similar form factors ($x/a = r/a = 1/2$) the results are very nearly the same in the two coordinate systems. Consequently, an average result will be quoted in this report, and no distinction between rectangular and cylindrical geometry will be maintained. It is expected also that all results will be correct in form in the analogous spherical geometry.

In Figs 4.2 and 4.3 average curves are plotted for a particular special case in order to illustrate the form of the step response and frequency response curves respectively. The case chosen is one in which the vessel dimension a

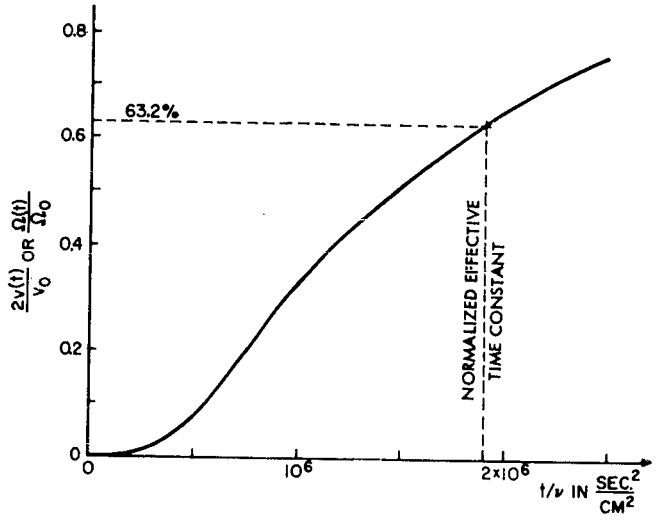

Fig. 4.2 Fluid System Step Response

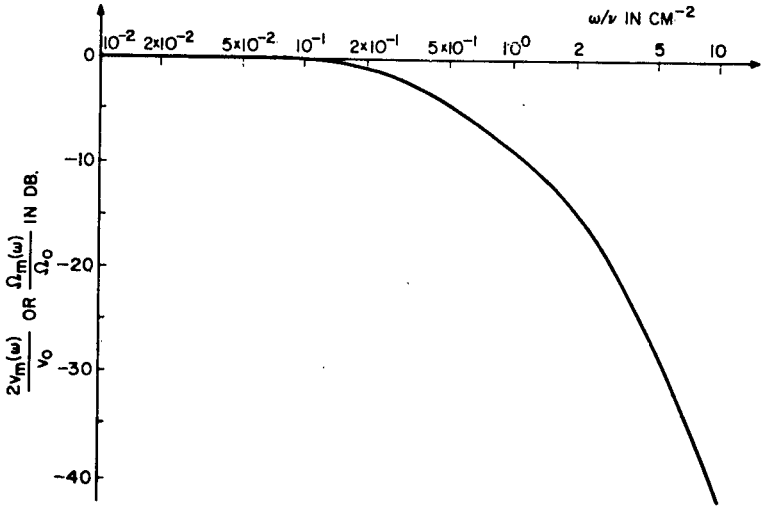

Fig. 4.3 Fluid System Frequency Response

is 5 cm, and the dimension at which the fluid motion is observed is x (or r) = 2.5 cm. (It will be noted from the step response solutions that the time constant governing the transient is proportional to a^2; a = 5 cm was chosen to be representative of an apparatus of moderate size.) In the curves shown, the time and frequency axes have been normalized in terms of the kinematic viscosity in order to make the results generally applicable to any fluid.

The inertial fixation of the fluid which is of interest is illustrated by the elapsed time interval before a response is observed in the step response transient of Fig. 4.2. This is not a true dead zone, but for the first 10^5 sec^2/cm^2 of normalized time the response is less than 0.15 percent of the final value; the fluid thus provides what can be considered an acceptable inertial reference during this interval. In real time this interval is inversely proportional to the kinematic viscosity of the chosen fluid, and thus the investigation turns to a study of this property in a number of fluids.

C. KINEMATIC VISCOSITY

Of the liquids investigated, mercury and ordinary water appear to be the most logical choices. The moderate viscosity and high density of mercury combine to give a kinematic viscosity at room temperature which is lower than that of all other unrefrigerated liquids studied, bettering the figure for water by a factor of 8. (At an elevated temperature of 60°C, the difference can be brought to within a factor of 5.) The coupling to the container is thus greater for water, but the suitability of water may not thereby be lessened since the factor of 13.6 difference in density between the two would allow a compensatory increase in vessel dimension in the case of water for a system of given weight.

In the initial search for fluids with low kinematic viscosity, attention was drawn to the "superfluid" liquid helium II, existing below 2.19°K. Study showed that although this fluid displays phenomena which can be interpreted in terms of a component with zero viscosity, this perfect lack of viscosity is invariably associated with thin films and narrow channels.[23] Specifically, the bulk liquid has a very small, but finite viscosity. Its kinematic viscosity is lower than that of any other known liquid, ranging

downward to perhaps 1×10^{-4} cm^2/sec as the temperature is lowered to the range between 1° and $1.5^{\circ}K$, but this figure only betters that for unrefrigerated mercury by a single order of magnitude.

It was questionable as to whether or not this single order of magnitude would justify the very considerable increase in apparatus complexity necessary to provide the extreme regrigeration required, but the study of liquid helium II was continued for a time and a property of this liquid was noted which settles clearly, and in the negative, the question of its suitability as a filling fluid for a liquid inertial reference system such as that which has been described.

In a manner not well understood, there is a rigidity associated with this fluid when it is rotating which is absent when it is at rest (just as it is absent in all classical fluids at all times). This phenomenon acts such as to make inapplicable the Navier-Stokes equation of motion in calculating the decay of rotation of fluid in a rotating vessel which is suddenly brought to a stop. There is, therefore, a fundamental nonlinearity which introduces a unilateral behavior into the system response. This is illustrated in quotations from two recent papers in which the drag torque on discs immersed in liquid helium II is measured by means of angular deflection of a quartz suspension.

> When rotation [of the cylinder] was started from rest a time delay was observed before any drag was seen, and the equilibrium drag was attained only after about one half hour. When rotation was stopped, the drag force immediately decreased, and the zero position was regained in a time much shorter than the build-up time.[24]

> A delay of several minutes elapses between setting the container suddenly into motion from rest and initial motion of the disc. In contrast, the disc responds immediately to stopping rotation of the vessel.[25]

The "time delay" to which both articles refer is exactly what one would expect the flat region at the foot of the step response to look like as observed at very low levels by an apparatus of finite sensitivity. The time constants reported in each case are consistent with the vessel dimensions used as

predicted by the step response solutions quoted in this report (corrected in a manner to be described later for the fact that their cylinder was of finite length in contrast to the infinite cylinder considered analytically). The immediate response to the stopping of rotation demonstrates that the rotating fluid is strongly coupled to the container walls and does not exhibit the decoupling necessary in an angular motion sensing device. In view of this, the study of liquid helium II was terminated.

Fluid	ν in $cm^2/sec.$
liquid helium II	$1 \times 10 - 7 \times 10^{-4}$
liquid hydrogen	1.6×10^{-3}
mercury 20°C	1.2×10^{-3}
60°C	1.0×10^{-3}
water 20°C	1.0×10^{-2}
60°C	4.8×10^{-3}

Fig. 4.4 Kinematic Viscosities of some Interesting Liquids

D. DEVICE CONFIGURATIONS--OPEN AND CLOSED LOOP OPERATION

In order to proceed further it will be convenient to introduce a standard notation which will be used hereafter. (see Fig. 4.5)

1. The motion of the fluid (specifically that portion of the fluid at some particular radius r) in inertial space will be measured by an angle θ_F.
2. The motion of the containing vessel in inertial space will be measured by an angle θ_c.
3. Relative motion between the container and the fluid, i.e., that motion which must be sensed, will be measured by an angle $\theta_\epsilon = \theta_c - \theta_F$.

An approximate open-loop system transfer function is found by fitting the frequency response curve of Fig. 4.3 with a second order Bode plot. (see Fig. 4.6). Such an approximation is useful in that it presents the essential behavior of the system

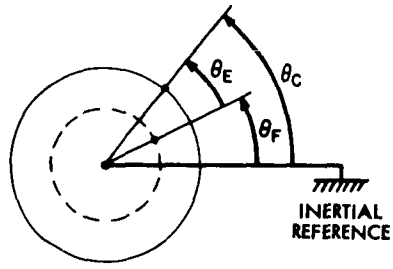

Fig. 4.5 Standard Notation for Angles

in a considerably simpler form than the analytical solutions of the equations of motion and allows investigation of system response to an arbitrary input function. It must be cautioned that the approximation is not accurate at small times corresponding to the high frequencies at which the second order plot departs from the actual frequency response, but this will not be a disadvantage in the present discussion.

In approximating the frequency response curve with a second order factor and using the approximate transfer function so derived to calculate various responses in the time domain, the assumption has been made implicitly that the system is minimum phase or can be so approximated to a satisfactory degree. Some assurance that this assumption is justifiable is provided in that a step response calculated using the approximate transfer function agrees quite closely with the step response given directly by the analytical solution of the Navier-Stokes equation--except, of course, at the small times mentioned in the caution above. While lacking in rigor, this approach will be sufficient for present purposes.

The transfer functions obtained in the manner above are

$$\frac{\theta_F(s)}{\theta_C(s)} = \frac{\alpha\beta}{(s+\alpha)(s+\beta)} \tag{4.5}$$

$$\frac{\theta_\epsilon(s)}{\theta_C(s)} = \frac{s(s+\alpha+\beta)}{(s+\alpha)(s+\beta)} \tag{4.6}$$

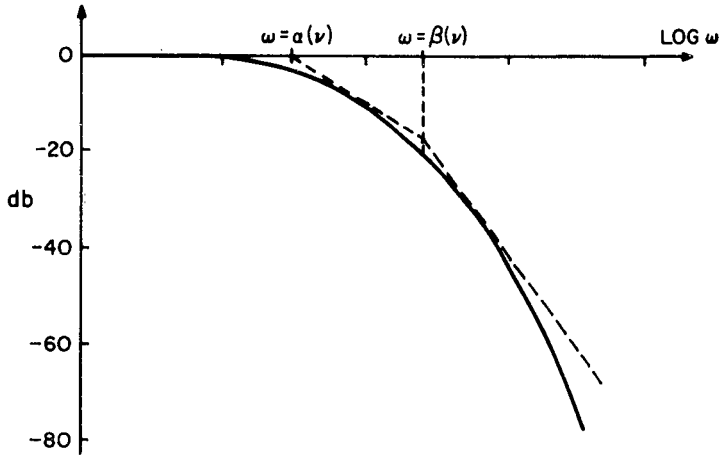

Fig. 4.6 Second Order Approximation to Open-Loop Response

where α and β are functions of ν since the curve has been plotted against actual angular frequency rather than normalized frequency.

Due to the fact that β exceeds α by almost an order of magnitude, the effective time constant of the system is given very closely by $\tau_{EFF.} = 1/\alpha$.

Consider the transfer function $\theta_\epsilon(s)/\theta_c(s)$ and suppose that the input motion of the container is a ramp of angle of slope Ω such that $\theta_c(s) = \Omega/s^2$. The form of the time response is shown in Fig. 4.7. The response curve in the time domain can conveniently be divided into two regions. For times very long compared with τ_{EFF} the device acts as a rate sensor, for the response in this region is proportional to the input angular rate Ω. For times which are a small fraction of τ_{EFF} the device acts as an angle sensor, the response being proportional to the actual angle θ_c through which the container has turned in inertial space. These two regions of the time response will be referred to as the regions of "rate" and "position" operation respectively.

One application of a device such as this would be as a rate sensor. In this application the device would be operated in the "rate" region of the response curve. Clearly, a rate would not be measurable by a device operating

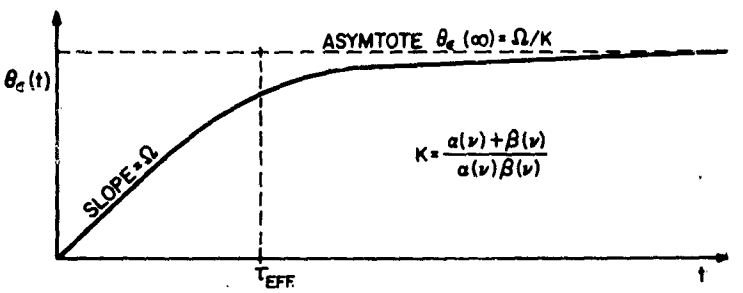

Fig. 4.7 Open-Loop Response to a Constant Angular Rate

in this mode until it had persisted unchanged over a length of time equal to several time constants. This considerable delay, amounting to 15 minutes or more for a system using mercury, together with the dependence of the calibration of the output upon an exact knowledge of the parameters α and β (which are strongly temperature dependent), make this type of open-loop operation unsatisfactory and it will not be considered further.

The alternative application is one in which the device is employed as an angle sensor and operation is confined to the position region of the response curve. This would in effect be inherently accomplished if the input were to contain no frequencies lower than a minimum which is perhaps an order of magnitude or two above β. For an arbitrary input containing low frequencies as well as high, however, operation within the position region can be insured only by closing a loop around the system. In the closed loop mode, any error angle θ_ϵ is driven to a null as soon as it appears. In this way, motion between the fluid and its container is not allowed to persist over a time longer than that required for the servo-mechanism transient, and if this transient is no more than a small fraction of τ_{EFF}, operation entirely within the position region has been accomplished.

Although it is not the intent of this report to consider in detail any implementation schemes taking advantage of the inertial fixation of the fluid, it is desirable at this point to discuss a system employing an elementary loop closure in order to illustrate the closed loop mode of

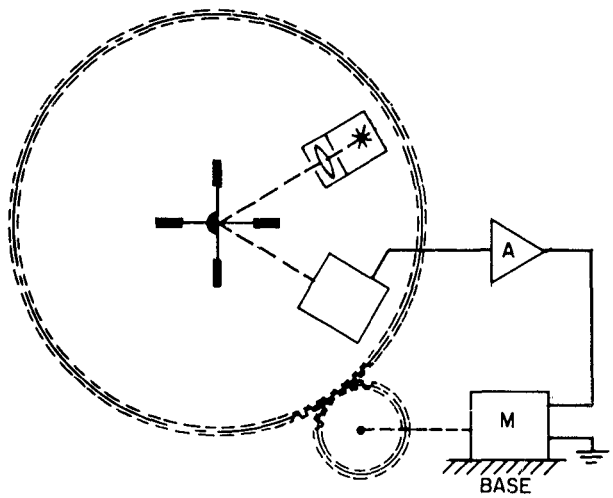

Fig. 4.8 A Possible Configuration for Closed-Loop Operation

operation in what it felt to be a representative manner. Such a system is shown in Fig. 4.8. In this system a convergent beam of light from a source which is fixed with respect to the container is reflected from a mirror mounted on the axis of symmetry and held fixed in the fluid by a paddle wheel arrangement. The focal plane of the reflected beam is a coded plate, and the associated electronics produce an electrical output proportional to the deviation from null. This output is amplified and applied to a motor which drives the error to zero. For such a system as this, the input can be considered to be the angle θ_B through which the base on which the entire system is mounted is turned (perhaps this is a vehicle which carries the inertial system). The object being to null the container with the fluid, the error angle is then θ_c. To assess the performance, the transfer function $\frac{\theta_c(s)}{\theta_B(s)}$ is written and the time function $\theta_c(t)$ determined for a test input. In order to simplify the expressions a number of approximations are made, notably that only a first order approximation to the open loop fluid transfer function is used and the motor is

represented as a pure integration. The closed loop transfer function, the test input and the resulting time response are shown below.

$$\frac{\theta_c(s)}{\theta_B(s)} = \frac{(s+a)}{(s+a+g)} \tag{4.7}$$

$$\theta_B(s) = \frac{\Omega_B}{s^2} \tag{4.8}$$

$$\frac{\theta_c(t)}{\Omega_B} \doteq \left[\left(\frac{a}{g}\right)t + \left(\frac{1}{g}\right)\left(1 - e^{-gt}\right)\right] u_{-1}(t) \tag{4.9}$$

where g represents the total gain around the loop.

It is seen that $\theta_c(t)$ is characterized by an offset angle and a constant drift rate, both proportional to the input angular velocity. Specification of a 45^o phase margin leads to a figure of 3.5×10^{-2} radians = 0.2 degrees for the offset angle and $3.5 \times 10^{-2}\ a(\nu)$ radians per second for the normalized drift rate, all per unit input angular velocity.

E. LOWER BOUND ON DETECTABLE RATE

An important performance index of a fluid angular motion sensing device is the minimum angular rate which it can detect, referred to hereafter as the MDR. This index is dependent in turn upon a characteristic of whatever sensing device is chosen to measure θ_ϵ, that being the minimum detectable angle or MDA. These limits did not arise in the last section since an ideal sensing device was assumed in which the electrical output was directly proportional to the error angle. In any actual device there will be a threshold angle below which there will be no output.

The relation between the MDA and the MDR can be deduced from the form of the open loop response curve of Fig. 4.7. That an MDR does indeed exist is apparent when it is realized that no rate can be detected which leads to a steady state offset angle which is less than the MDA. Moreover, it having been shown that a device which is of practical value must operate within the position region of the response curve, a more severe restriction is imposed by the fact that the MDA must be reached in a time which is a small fraction

of τ_{EFF}, say $\gamma\,\tau_{EFF}$. The mathematical expression for the relation between MDR and MDA is as below.

$$MDR = \left(\frac{k}{\gamma}\right) MDA \tag{4.10}$$

$$\text{where } k = \frac{a(\nu) + \beta(\nu)}{a(\nu)\quad \beta(\nu)}$$

That this is true is seen by the following argument. If the MDA is reached in a time $\gamma\,\tau_{EFF}$ when the input rate is Ω = MDR, then $\frac{MDA}{\gamma}$ will be reached in time τ_{EFF} at this rate on a linearly extropolated curve. However, the geometry shows that the angle reached in time τ_{EFF} at this rate Ω = MDR is $\frac{MDR}{k}$. Equating the angles then gives

$$\frac{MDA}{\gamma} = \frac{MDR}{k} \tag{4.10a}$$

or

$$MDR = \frac{k}{\gamma}\ MDA \tag{4.10}$$

As noted previously, the second order approximation to the system transfer function is not accurate for small values of time, and thus the deviation from strictly proportional behavior as a function of γ is calculable only directly from the full analytic solutions. Such a calculation has been performed, and the result appears in Table 4.1.

γ	% deviation from linearity
0.35	5 %
0.30	3 %
0.25	2 %
0.20	1 %
0.15	0.4 %
0.10	0.1 %

Table 4.1 Percentage Deviation from Linearity as a Function of γ.

F. SUMMARY OF DEVICE PERFORMANCE

By considering a vessel of dimensions r = 2.5 cm, a = 5 cm and substituting into the analytical solutions the values of the kinematic viscosity for mercury and for water at 20°C, the values in Table 4.2a are obtained.

	H_2O	Hg
α	4.6×10^{-3}	5.5×10^{-4}
β	3.2×10^{-2}	3.9×10^{-3}
$k = \frac{\alpha+\beta}{a\beta}$	4.1×10^{-3}	4.8×10^{-4}
τ_{EFF}	265 sec.	2200 sec.

a

	H_2O	Hg
α	3.3×10^{-2}	4.0×10^{-3}
β	2.3×10^{-1}	2.8×10^{-2}
k	2.9×10^{-2}	3.5×10^{-3}
τ_{EFF}	30 sec.	250 sec.

b

Table 4.2. Parameters for Water and for Mercury in a Vessel of Dimension r = 2.5 cm, a = 5 cm at a Temperature of 20°C.
a) Theoretical
b) Attainable

Table 4.2b shows more realistic figures which are based on the use of a finite apparatus rather than the infinite cylinder assumed in the analytical solution. The deterioration from the values of part a is roughly by a factor of 8. This factor is rather larger than would be expected on the basis of end effects alone, but it is felt to be representative of what deterioration might be encountered in practice, for whatever reason. Its size was determined by a series of relatively crude experiments which measured the effective time constant of the step response of an apparatus filled with water, and the resulting value was further corroborated, at least in order of magnitude, by the data obtained in the experiments of Craig and Pellam quoted in Section C of this chapter. The chosen factor of 8 abstracted from this empirical evidence

is conservative.

Insertion of the figures from Table 4.2b into the simplified expression for closed loop error time response (Eq. 4.9) leads to expected values of the drift rate per unit angular velocity input (in radians/sec) of 1.2×10^{-3} and 1.4×10^{-4} radians/sec for water and mercury respectively. It will be remembered that these figures apply to an elementary loop closure employing only pure gain compensation, but they are illustrative of what can be attained. That these rates appear to be quite high with respect to an earth rate is to some extent an improper criticism of the system since these drift rates are proportional to the input angular rate. A more meaningful statement of capability is perhaps that drift rates are 0.12% and 0.014% of a constant input rate for water and for mercury respectively.

The drift rates are applicable so long as the input angular rate does not fall below the MDR defined in the previous section. Since the effective time constants of Table 4.2b are a great deal larger than the duration of transients in any servomechanism which would be involved in the loop closure, it is seen that very small values of δ, corresponding to negligible deviations from linearity are within reach, particularly in the case of mercury. Choosing $\delta = 0.10$, the MDR per unit MDA is 0.29 radians/sec per radian for water and 0.035 radians/sec per radian for mercury. In terms of earth rates and angle sensitivity in degrees these figures become 70 earth rates/degree and 8.6 earth rates/degree respectively. Since the simple closed loop system and optical sensing means described previously can be made to have an angle detection capability giving an MDA or 0.005° without difficulty and in a reasonably small package, this device could be expected to exhibit a rate detection capability down to an MDR of 0.35 earth rate for water and 0.043 earth rate for mercury for this choice of δ.

G. CONCLUSIONS

It is felt that the indications of expected performance given in the previous section are sufficiently good to justify the conclusion that a fluid-filled angular motion sensing device of the type described, using mercury as the fluid, and employed in a closed loop mode of operation can satisfactorily meet the first criterion of success, that being that the fluid does remain sensibly fixed in

inertial space over usefully long times when the system is subjected to practical input motions. This criterion is met only marginally for water, but the possible use of an elevated temperature (60°C) and the large difference in density between the two fluids can materially improve the suitability of water as remarked in Section C of this chapter.

The first criterion having been shown to have been met, it is concluded further that a study of sensing devices designed to detect relative motion between the fluid and its container might profitably be initiated. In order to be of real value, such a sensor must be suitable for use in the spherical geometry where inputs around any arbitrary axis could be detected, in contrast to the illustrative sensor described in this report which is sensitive about a single input axis.

REFERENCES

1. W. M. Siebert. "Notes on Modern Network Theory".

2. International Telephone and Telegraph Company: Reference Data for Radio Engineers, (fourth edition).

3. Culver, W. H. "Nuclear Gyros," American Rocket Society Paper No. 1948-61, presented at the Guidance, Control and Navigation Conference, Stanford University, August, 1961.

4. Bloch, F. "Nuclear Induction," Physical Review, vol. 70, p. 460 (1946).

5. Rabi, Ramsey, and Schwinger. "Use of Rotating Coordinates in Magnetic Resonance Problems," Reviews of Modern Physics, vol. 26, p. 167 (1954).

6. Abragam, A. The Principles of Nuclear Magnetism Oxford University Press (1961).

7. Andrew, E. R. Nuclear Magnetic Resonance, Cambridge University Press (1956).

8. Simpson, J. H. "Interim Technical Note on Nuclear Gyroscope Study," General Precision Laboratories (sponsored by WADC). (CONFIDENTIAL)

9. Abragam, A. "Overhauser Effect in Nonmetals." Physical Review, vol. 98 p. 1729 (1955).

10. Abragam, A., Combrisson, J., and Solomon, I. "Polarization Nucleaire par effet Overhauser dans les solutions d'ions paramagnetiques," Comptes Rendus de l' Academie des Sciences, vol. 245 p. 157 (1957).

11. Gannsen, A., and Sloan, E. L. "Spectral purity test of the proton RASER oscillator", presented at the American Physical Society meeting at New York City, 24 January 1962.

12. Gordon, J. P; Zeiger, H. J; and Townes, C. H. "The MASER-new type of microwave amplifier, frequency standard, and spectrometer," Physical Review, vol. 99, p. 1264 (1955).

13. Shoenberg, D: Superconductivity, Cambridge University Press, 2nd Edition (reprinted 1960).

14. Meissner, W. and Ochsenfeld, R., Naturwissenshaften, vol. 21 p. 787 (1933).

REFERENCES (continued)

15. Barnes, F. S. "A Magnetic Shield for Beam Frequency Standards," Proceedings of the I. R. E., vol. 49, p. 1328 (1961).

16. Deaver, B. S., Jr. and Fairbank, W. M. "Experimental Evidence for Quantized Flux in Superconducting Cylinders," Physical Review Letters, vol. 7, p. 43 (July 15, 1961).

17. London, F. Superfluids, vol. I, New York, Wiley (1950).

18. Weiser, Colloidal Chemistry, p. 207, Wiley and Sons, New York

19. Adamson, Surface Chemistry, Wiley and Sons, New York

20. Hartman, Colloidal Chemistry, p. 257, Riverside Press, Cambridge, Mass.

21. Dorn, Wied Ann., vol. 10, p. 46 (1880).

22. Franklin, P., Methods of Advanced Calculus, First Edition, McGraw-Hill (1944).

23. Atkins, K. R., Liquid Helium, Cambridge University Press, (1959).

24. Craig, P. P. "Drag Forces in Rotating He II," Physical Review Letters, vol. 7, No. 9, November 1, 1961.

25. Pellam, J. R., "Evidence on the Nature of Rotating Liquid Helium," Physical Review Letters, vol. 5, No. 5, September 1, 1960.

Aeronautical Systems Division, Dir/Avionics, Navigation and Guidance Lab, Wright-Patterson AFB, Ohio. Rpt No. ASD-TDR-62-492, Vol II. THEORETICAL INVESTIGATION OF A MAGNETO-OPTICAL GYROSCOPE: Alternatives to the Faraday Effect. Final report, Feb 63, 78p. incl illus., tables, 25 refs.

Unclassified Report

This report summarizes a theoretical investigation of the feasibility of using magneto-optical and certain other physical phenomena for gyroscopic measurement purposes. The phenomena investigated in this report are nuclear angular momentum effects, Coriolis force effects on various particles and bulk fluid effects. This report supplements Report ESL-R-125(I) which presents results of an investigation of magneto-optical and other closely related phenomena. The overall investigation, including the researches of both the previous report and this supplement, is summarized

(over)

in Chapter I of this report.

The conclusions reached are as follows. The magneto-optical gyroscope, based on the Barnett and Faraday effects, is potentially capable of a resolution on the order of 0.1 radian per second providing stray magnetic field effects are shielded to maintain field fluctuations down to the order of 10^{-9} gauss. Methods based on nuclear angular momentum may be able to achieve one *to three orders of magnitude more resolution with less* sensitivity to stray fields than the magneto-optical approach. Maser techniques would be needed to reach the lower limit on resolution. Coriolis force effects in specially constructed dielectrics appear to be too small in comparison with other forces to be useful. This conclusion applies to both microscopic and colloidal particle sizes. The investigation closed with a study of bulk fluid effects. It is shown that an ordinary liquid like mercury is sufficiently decoupled from its container so that it may be useful as a stable platform reference. However, the problem has not been solved.

1. Inertial guidance
2. Gyroscopes
I. AFSC Project 4431, Task 443124
II. Contract AF33(616)-7668
III. Electronic Systems Lab, Department of Electrical Engineering, Massachusetts Institute of Technology, Cambridge 39, Mass.
IV. ESL-R-125(II)
V. Aval fr OTS
VI. In ASTIA collection

Aeronautical Systems Division, Dir/Avionics, Navigation and Guidance Lab, Wright-Patterson AFB, Ohio. Rpt No. ASD-TDR-62-492, Vol II. THEORETICAL INVESTIGATION OF A MAGNETO-OPTICAL GYROSCOPE: Alternatives to the Faraday Effect. Final report, Feb 63, 78p. incl illus., tables, 25 refs.

Unclassified Report

This report summarizes a theoretical investigation of the feasibility of using magneto-optical and certain other physical phenomena for gyroscopic measurement purposes. The phenomena investigated in this report are nuclear angular momentum effects, Coriolis force effects on various particles and bulk fluid effects. This report supplements Report ESL-R-125(I) which presents results of an investigation of magneto-optical and other closely related phenomena. The overall investigation, including the researches of both the previous report and this supplement, is summarized

(over)

in Chapter I of this report.

The conclusions reached are as follows. The magneto-optical gyroscope, based on the Barnett and Faraday effects, is potentially capable of a resolution on the order of 0.1 radian per second providing stray magnetic field effects are shielded to maintain field fluctuations down to the order of 10^{-9} gauss. Methods based on nuclear angular momentum may be able to achieve one *to three orders of magnitude more resolution with less* sensitivity to stray fields than the magneto-optical approach. Maser techniques would be needed to reach the lower limit on resolution. Coriolis force effects in specially constructed dielectrics appear to be too small in comparison with other forces to be useful. This conclusion applies to both microscopic and colloidal particle sizes. The investigation closed with a study of bulk fluid effects. It is shown that an ordinary liquid like mercury is sufficiently decoupled from its container so that it may be useful as a stable platform reference. However, the problem has not been solved.

1. Inertial guidance
2. Gyroscopes
I. AFSC Project 4431, Task 443124
II. Contract AF33(616)-7668
III. Electronic Systems Lab, Department of Electrical Engineering, Massachusetts Institute of Technology, Cambridge 39, Mass.
IV. ESL-R-125(II)
V. Aval fr OTS
VI. In ASTIA collection

Aeronautical Systems Division, Dir/Avionics, Navigation and Guidance Lab, Wright-Patterson AFB, Ohio. Rpt No. ASD-TDR-62-492, Vol II. THEORETICAL INVESTIGATION OF A MAGNETO-OPTICAL GYROSCOPE: Alternatives to the Faraday Effect. Final report, Feb 63, 78p. incl illus., tables, 25 refs.

Unclassified Report

This report summarizes a theoretical investigation of the feasibility of using magneto-optical and certain other physical phenomena for gyroscopic measurement purposes. The phenomena investigated in this report are nuclear angular momentum effects, Coriolis force effects on various particles and bulk fluid effects. This report supplements Report ESL-R-125(I) which presents results of an investigation of magneto-optical and other closely related phenomena. The overall investigation, including the researches of both the previous report and this supplement, is summarized

(over)

in Chapter I of this report.

The conclusions reached are as follows. The magneto-optical gyroscope, based on the Barnett and Faraday effects, is potentially capable of a resolution on the order of 0.1 radian per second providing stray magnetic field effects are shielded to maintain field fluctuations down to the order of 10^{-9} gauss. Methods based on nuclear angular momentum may be able to achieve one to three orders of magnitude more resolution with less sensitivity to stray fields than the magneto-optical approach. Maser techniques would be needed to reach the lower limit on resolution. Coriolis force effects in specially constructed dielectrics appear to be too small in comparison with other forces to be useful. This conclusion applies to both microscopic and colloidal particle sizes. The investigation closed with a study of bulk fluid effects. It is shown that an ordinary liquid like mercury is sufficiently decoupled from its container so that it may be useful as a stable platform reference. However, the problem has not been solved.

1. Inertial guidance
2. Gyroscopes
I. AFSC Project 4431, Task 443124
II. Contract AF33(616)-7668
III. Electronic Systems Lab, Department of Electrical Engineering, Massachusetts Institute of Technology, Cambridge 39, Mass.
IV. ESL-R-125(II)
V. Aval fr OTS
VI. In ASTIA collection

Aeronautical Systems Division, Dir/Avionics, Navigation and Guidance Lab, Wright-Patterson AFB, Ohio. Rpt No. ASD-TDR-62-492, Vol II. THEORETICAL INVESTIGATION OF A MAGNETO-OPTICAL GYROSCOPE: Alternatives to the Faraday Effect. Final report, Feb 63, 78p. incl illus., tables, 25 refs.

Unclassified Report

This report summarizes a theoretical investigation of the feasibility of using magneto-optical and certain other physical phenomena for gyroscopic measurement purposes. The phenomena investigated in this report are nuclear angular momentum effects, Coriolis force effects on various particles and bulk fluid effects. This report supplements Report ESL-R-125(I) which presents results of an investigation of magneto-optical and other closely related phenomena. The overall investigation, including the researches of both the previous report and this supplement, is summarized

(over)

in Chapter I of this report.

The conclusions reached are as follows. The magneto-optical gyroscope, based on the Barnett and Faraday effects, is potentially capable of a resolution on the order of 0.1 radian per second providing stray magnetic field effects are shielded to maintain field fluctuations down to the order of 10^{-9} gauss. Methods based on nuclear angular momentum may be able to achieve one to three orders of magnitude more resolution with less sensitivity to stray fields than the magneto-optical approach. Maser techniques would be needed to reach the lower limit on resolution. Coriolis force effects in specially constructed dielectrics appear to be too small in comparison with other forces to be useful. This conclusion applies to both microscopic and colloidal particle sizes. The investigation closed with a study of bulk fluid effects. It is shown that an ordinary liquid like mercury is sufficiently decoupled from its container so that it may be useful as a stable platform reference. However, the problem has not been solved.

1. Inertial guidance
2. Gyroscopes
I. AFSC Project 4431, Task 443124
II. Contract AF33(616)-7668
III. Electronic Systems Lab, Department of Electrical Engineering, Massachusetts Institute of Technology, Cambridge 39, Mass.
IV. ESL-R-125(II)
V. Aval fr OTS
VI. In ASTIA collection